Since January 2020 Elsevier has created a COVID-19 resource centre with free information in English and Mandarin on the novel coronavirus COVID-19. The COVID-19 resource centre is hosted on Elsevier Connect, the company's public news and information website.

Materials Today Advances 14 (2022) 100214

Contents lists available at ScienceDirect

Materials Today Advances

journal homepage: www.journals.elsevier.com/materials-today-advances/

Calcium carbonate vaterite particles for drug delivery: Advances and challenges

Daria B. Trushina [a, b], Tatiana N. Borodina [a], Sergei Belyakov [c], Maria N. Antipina [d, *]

[a] A.V. Shubnikov Institute of Crystallography of Federal Research Centre "Crystallography and Photonics" of Russian Academy of Sciences, Russian Academy of Sciences, Moscow, 119333, Russia
[b] I.M. Sechenov First Moscow State Medical University, Moscow, 119991, Russia
[c] Theracross Technologies Pte Ltd, 251 Pasir Panjang Rd, Singapore, 118610, Singapore
[d] Singapore Institute of Food and Biotechnology Innovation A*STAR, 31 Biopolis Way, #01-02 Nanos, Singapore, 138669, Singapore

ARTICLE INFO

Article history:
Received 15 December 2021
Accepted 1 February 2022
Available online 12 February 2022

Keywords:
Vaterite
Drug delivery
Loading methods
Loading capacity
Multi-drug loading
Tumor-targeting

ABSTRACT

The recent successful application of lipid-based nanoparticles as delivery vehicles in COVID-19 vaccines demonstrated the superior potential of nanoparticle-based technology for targeted drug delivery in biomedicine. Among novel, rapidly advancing delivery platforms, the inorganic nano/microparticles gradually reach new heights and attract well-deserved attention among scientists and clinicians. Calcium carbonate in its vaterite form is used as a biocompatible carrier for a progressively increasing number of biomedical applications. Its growing popularity is conferred by beneficial porosity of particles, high mechanical stability, biodegradability under certain physiological conditions, ability to provide a continuous steady release of bioactives, preferential safety profile, and low cost, which make calcium carbonate a suitable entity of highly efficacious formulations for controlled drug delivery and release. The focal point of the current review is the success of the recent vaterite applications in the delivery of various diagnostics and therapeutic drugs. The manuscript highlights the nuances of drug loading in vaterite particles, connecting it with particle morphology, size, and charge of the loaded molecules, payload concentration, mono- or multiple drug loading. The manuscript also depicts recent successful methods of increasing the loading capacity developed for vaterite carriers. In addition, the review describes the various administration routes for vaterite particles with bioactive payloads, which were reported in recent years. Special attention is given to the multi-drug-loaded vaterite particles ("molecular cocktails") and reports on their successful delivery *in vitro* and *in vivo*.

1. Introduction

The development of novel particle-based formulations for targeted drug delivery is significantly hurdled upon transferring the technology from the lab to the market by high fabrication costs, complicated scale-up, potential material safety issues, and laborious procedures to get approval from drug administration authorities. Among all the existing drug delivery systems, liposomal formulations are perhaps the most successful, considering their therapeutic efficacy and market invasion. It was predicted in the pre-COVID-19 world that the global liposome drug delivery market would reach ~ USD 7.00 billion by 2027, but with hurdles and setbacks associated with pandemic-struggling economy, the number was adjusted to the more modest value due to a decline of the liposome market in 2020. However, this market segment is predicted to jump up again, considering the overall success of lipid-nanoparticle-based vaccines for COVID-19 in 2021.[1] It should be noted that currently marketed non-invasive drug delivery systems do not employ liposome-based formulations – these do almost entirely belong to the range of parenteral administration protocols. Oral delivery of liposome-based drugs is heavily affected by their propensity to collapse in highly aggressive gastro-intestinal

* Corresponding author.
E-mail addresses: trushina.d@mail.ru (D.B. Trushina), astra44@list.ru (T.N. Borodina), belyakov_s@yahoo.com (S. Belyakov), Maria_Antipina@sifbi.a-star.edu.sg (M.N. Antipina).

[1] Online. 2021 August. Available from URL: https://www.globenewswire.com/news-release/2021/02/02/2167962/28124/en/Global-Liposomal-Drug-Delivery-Devices-Market-Report-2020-Market-is-Expected-to-Recover-and-Reach-4-43-Billion-in-2023-at-a-CAGR-of-10-27-Forecast-to-2030.html.

https://doi.org/10.1016/j.mtadv.2022.100214

surroundings (bile salts, lipases, low pH), problems with biomembrane crossing, inherent toxicity of lipid-based nanoparticles assembled from positively charged lipids, etc. [1].

On the other hand, the liposome-based drug production cost is 100-times higher than conventional non-liposomal drugs [2,3]. It is reported that high acquisition costs of the existing nanoformulations may prevent their large-scale use since the traditional drug forms turned out to be by far more affordable [4]. Many efforts have been made to accelerate the development of cost-effective nanomedicine, and a few alternative delivery vehicles have been designed and proposed. Among them, mineral particles such as clay, halloysite, calcium apatite, and calcium carbonate [5,6] have found use in various biomedical applications thanks to unique mechanical, physical, and chemical properties, low toxicity, biocompatibility, and/or biodegradability [6–9]. The production costs for such materials are significantly lower than those for liposomes or metal nanoparticles: the estimated cost for 1 g of halloysite or calcium carbonate is only 0.2–0.4 USD, whereas 1 g of liposomes can cost more than 100 USD [5].

$CaCO_3$ particles in vaterite modification stand out of the range of mineral alternatives and other anhydrous calcium carbonate polymorphs considering the scope of potential applications in biomedicine, including drug delivery. The porous morphology and developed internal structure of vaterite allow hosting molecules of diverse nature. These particles can effectively entrap a wide variety of bioactive substances, including low molecular weight compounds and macromolecules, loaded into vaterite by physical adsorption (diffusion) into pores or co-precipitation (co-synthesis) during the particle formation. Variable size and pH-sensitive property of vaterite particles facilitate their use for controlled drug and gene delivery. The additional and quite appealing benefit of vaterite as a delivery vehicle is the targeted cancer therapy exploiting the enhanced permeability and retention (EPR) effect for penetration of the tumor followed by the vehicle degradation and release of payload in the acidic environment of cancer cells [10,11]. The high affinity of the vaterite crystals to mucin [12] holds a high promise for developing the vaterite-based mucosal drug delivery systems [13]. Thus, recent reports demonstrate intranasal [14], ocular [15], and pulmonary [16] delivery of the vaterite particles. At the same time, transdermal [17] and oral [18] administration of therapeutic molecules using vaterite are of particular scientific interest, which most certainly will become an attractive trait for industrial applications.

Unlike other popular drug delivery agents, such as metal nanoparticles, synthetic copolymers, and cationic lipids, calcium carbonate has no potential issues with material safety and is already marketed as an FDA-approved antacid (sec. 331.11b), digestive, antidiarrheal, and weight control drug (sec. 310.545), thus facilitating the approvals and implementation of novel vaterite-based drug formulations.

The scope of the current review covers the utility and efficiency of calcium carbonate in its vaterite polymorph for multiple aspects of drug delivery *in vivo*. The manuscript goes over various loading methodologies employing both single and multicomponent payloads and provides an overview of the methods to increase loading. The formulation design principles are discussed for injections and other parenteral and oral administration routes. The delivery systems for non-injectable administration are generally preferred by patients with higher compliance primarily because of the alleviation of pain during the drug delivery process and the possibility of outpatient self-administration. In the current review, additional attention is given to the methods utilizing multicomponent delivery systems based on vaterite, as this approach offers substantial benefits in targeted treatment using the synergistic effect of several drugs in a single particle. The use of vaterite for delivery of such "drug cocktails" favorably positions vaterite over other delivery systems, e.g., liposomes, polymersomes, and metal-based nanoparticles lacking porosity.

2. Drug loading

2.1. Loading capacity and loading efficacy

The amount of active substance is the most critical parameter for encapsulated drug forms to determine the therapeutic dosage. A common way to characterize the drug loading is to estimate either a weight percent of drug in the delivery system (loading capacity, LC) or a percentage of the entrapped drug to its initial amount used for loading (loading efficacy, LE).

LE varies substantially on the initial concentration of a drug substance and the delivery system's volume capacity; it is mainly used to judge the effectiveness of developed encapsulation protocol. Optimization of LE is essential to reduce losses of active compounds or drugs by minimizing the amounts left behind during the loading process. On the other hand, LC is exactly the parameter needed to estimate the encapsulated drug dosage before administration *in vitro* or *in vivo*. The loading protocol optimized for the maximal LC ensures the minimal amount of the delivery system particles to enter a cell or a body, reducing the systemic and local toxicity of the carrier material or its components. Apart from the loading conditions, both LE and LC depend on the properties of the delivery system, including the volume, surface area, reactivity with the drug molecules, etc. These parameters are not interconnected, and quite frequently, both LE and LC are provided in the published data to characterize the delivery system and the loading process alike. In this review, the loading of vaterite will be mainly discussed from the viewpoint of LC to reflect the ability of this carrier to incorporate drugs into its porous matrix.

Although the details do vary, there are two generally accepted approaches to obtain drug-loaded $CaCO_3$ [19]: 1) precipitation of $CaCO_3$ in the single- or double-phase [18] medium containing a dissolved or dispersed drug, and 2) surface adsorption and pore penetration of drug molecules onto pre-synthesized vaterite particles, which can be facilitated by different means, e.g., by freezing [20,21].

Co-precipitation of vaterite and drug often results in higher loading for water-soluble compounds [13,22,23]. However, certain drug molecules may create a preference for a particular shape and size of the forming vaterite particles [24]. Besides, drugs subjected to high ionic strength and pH changes upon vaterite formation may experience a dramatic loss of activity [23]. The issue with particle morphology preference can be addressed by co-precipitation of payload with molecules promoting the formation of vaterite particles with specific parameters. For example, poly(styrene sulfonate) was successfully used in the co-precipitation of vaterite and curcumin to grant the formation of particles of the desired size, i.e., 500 nm [25].

Surface adsorption of drug molecules and entrapment within the pores of vaterite particles is a way to avoid the drawbacks of the co-precipitation method mentioned above. Since vaterite is stable in non-polar media, the surface adsorption approach opens up a possibility to load hydrophobic compounds that are initially dissolved in organic solvents. By using the adsorption method, various compounds with potential anticancer activity and chemotherapeutics, e.g. curcumin (LC = 2.3 wt% [25]), camptothecin (LC = 0.0015 wt% [26]), cisplatin (LC = 0.05 wt% [27]), and paclitaxel (LC = 0.09 wt% [28]) were loaded into porous $CaCO_3$.

An attempt to link the polarity of the solvent as a function of drug solubility and, respectively, as a mean for altered drug loading into porous $CaCO_3$, using ibuprofen and several organic solvents

was made [29]. However, while this represents an interesting technological approach, the actual results should be interpreted differently. According to the authors [29], the LC of vaterite for ibuprofen increased with decreasing the solvent polarity and reached a maximum at 0.087 wt% of drug adsorbed from its solution in hexane. This work closely follows the experimental protocol and results of the previous study done with mesoporous silica as the carrier [30] and the same set of solvents. In both works, other solvents used had much higher polarity. Yet, at the same time, they had the higher solubility toward ibuprofen and (what is essential for the experiment details provided, since the evaporation of the solvents was done at 40 °C) much higher boiling points, which led to the leftovers of the solvents in the pores and, respectively, to the higher chance of the drug being removed together with these residual solvents in the $CaCO_3$ crevices upon successive washing with ethanol before measurements.

Feoktistova et al. [31] made a direct comparison of the co-precipitation and adsorption methods regarding their impact on the loaded molecules' bioactivity. The authors demonstrated that catalase activity decreased by 70% and 20% upon loading via the co-precipitation and adsorption method, respectively. The significant activity loss during the co-precipitation method, per authors, was a result of the alkaline-induced denaturation and aggregation of the enzyme molecules induced by calcium ions. However, recent studies in this area revealed that the co-precipitation method could be optimized to prevent an effect of the imminent basicity and respective rapid decrease in the functional molecule bioactivity. For example, Binevski et al. [15] suggested using a pH buffer for co-synthesis; this improvement to otherwise classical routine resulted in an increased content of superoxide dismutase in the vaterite microparticles (24 wt% after synthesis in the TRIS buffer at pH 8.4 vs. 15 wt% after synthesis in pure water at pH 10.3) and in order of magnitude higher enzymatic activity compared to synthesis in water. Another important observation of this study revealed that the TRIS buffer had no impact on the morphology of vaterite microcrystals. She et al. [32] and Kakran et al. [33] showed earlier that the use of PBS and TRIS buffers alongside the "molecular protectors" of functional macromolecules such as FGF2 and mRNA allows to co-precipitate them with $CaCO_3$ without loss of activity of respective bioactives.

For more chemically stable molecules, like typical photodynamic therapy (PDT) drugs, co-precipitation remains a preferential loading method granting a higher LC. Typically, the LC of the vaterite particles with a diameter of 0.7 μm for Photosens adsorption method (a mixture of sulfonated aluminum phthalocyanines) is in the range of 1.4 ± 0.4 wt% [34]. However, co-precipitation of this drug with $CaCO_3$ resulted in the formation of the 0.9 μm vaterite microparticles containing reasonably higher LC (2.0 ± 0.2 wt%) of Photosens [35]. Similar to the above-mentioned synthetic molecules, water-soluble herbal extracts of *Plantago major* and *Calendula officinalis* L. were loaded with higher LC by co-precipitation *vs.* adsorption technique [36]. The respective multilayer capsules assembled on the loaded vaterite templates (followed by the template dissolution) showed a preferential acceleration of mucosal healing of the stomach in rats.

LC of the vaterite particles can be determined by two approaches: i) indirectly, by measuring the concentration of the payload remaining in the supernatant after loading, or ii) directly, by measuring the concentration of the payload in the medium after the dissolution of $CaCO_3$. Although both approaches are accepted and implemented widely, the direct measurement of LC seems to be more reliable for applications requiring a precise dosage estimation since there is conclusive evidence of the loading overestimation in the indirect approach. One of the typical examples includes the immobilization of alkaline phosphatase on vaterite microparticles, varying the particle size, enzyme concentration, and adsorption time [37]. At specific conditions equal for both approaches, the indirectly measured LC is noticeably higher than the direct LC assessment, i.e., 44–48 wt% vs. 16–20 wt%, respectively.

Achieving the maximum LC requires thorough optimization of a series of parameters, such as the concentrations of salts and/or active molecules, concentrations of co-encapsulants in the co-precipitation method, the number, size, and porosity of vaterite particles, the concentration of payload, solvent type, pH and the overall system ionic strength in the adsorption method. Such a multitude of parameters is hard to expect to be reported exhaustively in a single research manuscript; more so, there are no shortened sets of generally accepted parameters and proven reliable for a confident comparison of the data from different sources.

The factors influencing co-precipitation are closely related to the morphology of the forming $CaCO_3$ crystals [24,38]. These factors are extremely complex and are comprehensively reported in the literature; therefore, they are worth a separate review. This manuscript will give a brief account of the most commonly reported parameters impacting particle loading via the adsorption method.

2.1.1. Impact of the particle morphology

The morphology of $CaCO_3$ vaterite particles may vary drastically depending on the synthesis conditions. The obtained particles do have different shapes, sizes, and porosities. Here again, the selection of so-called "key factors" is often deviating from paper to paper but overall is relatively well-studied (see, for example, [39]. The surface area, pore volume, and pore size are usually the typical parameters impacting the LC of the particles.

While loading human guanylate kinase (23 kDa) in vaterite particles of different shapes, Donatan et al. [40] reported a higher adsorption efficiency for star-shaped particles compared to elliptical and spherical ones (4.8 wt% vs. 2.8–4.0 wt%). The obtained LC values correlated directly with the surface area of the studied particles. A similar trend of the lowest loading with TRITC-dextran (70 kDa) was observed elsewhere [41] for spherical vaterite compared to star-like and elliptical particles possessing higher surface areas.

Smaller particles have a higher surface area than their larger counterparts, and therefore, it seems logical to expect a reversed relation between the particle size and LC, assuming no major difference in porosity. In line with this statement, Parakhonskiy et al. [41] have observed a higher LC for TRITC-dextran (70 kDa) of 0.6 μm spherical vaterite, which was twice as high as of the particles 3.6 μm (10×10^{-3} wt% vs. 5×10^{-3}, respectively). Vikulina et al. [42] demonstrated an even stronger tendency: co-precipitation of lysozyme (14.3 kDa) with $CaCO_3$ resulted in loading of 0.5 g of the enzyme per 1 g of 1 μm spherical vaterite, while only 0.045 g of lysozyme was incorporated in 1 g of 15–25 μm $CaCO_3$ particles. On the contrary, Donatan et al. [40] have found no correlation between the size and the loading of spherical particles with a diameter of 1–3 μm. The obtained LC values varied just slightly and were in the range of $8–10 \times 10^{-3}$ wt%. These data may seem to favor the absence of the trend, but one essential difference between the two results is hidden in the apparent particle polydispersity, which is common for precipitated $CaCO_3$. This suggestion is supported by the fact that the same authors [40] have reported an increase in the LC by TRITC-dextran (70 kDa) for elliptical $CaCO_3$ particles as a function of decreasing the particle size from 2.1×1.3 μm to 1.5×0.7 μm. The respective LC data were obtained as 5×10^{-3} and 9×10^{-3} wt%.

Cyanine 7 NHS ester (Cy7), a low molecular weight (Mw = 733.64) water-insoluble fluorescent dye, was loaded in vaterite particles of three different sizes: 0.65 μm, 1.35 μm, and 3.15 μm from a DMSO solution [16]. The obtained LCs had a distinct

trend to decrease with increasing the particle size and were estimated as 10.3 wt%, 1.5 wt%, and 0.88 wt%, respectively. Interestingly, a much higher loading of a hydrophobic substance was achieved from the solution in DMSO in this case than compared to ibuprofen loading using the DMSO solution [29], which again underlines the importance of accounting for multiple factors, including boiling point and vapor pressure of the solvents.

However, small particle size doesn't always grant a high LC. For instance, the maximum LC of a photosensitizer, Hypocrellin B, from acetone for vaterite (250 nm particle size) co-precipitated with gelatin was as low as 0.02 wt% [43]. The possible reason for this effect could be a fairly low drug concentration (0.5 mg/mL, 1 mg/mL, 1.5 mg/mL, and 2 mg/mL) and non-optimized concentration of the particles upon loading. Unfortunately, the cited paper lacks data relevant to the particle pore volume, which could be drastically decreased by gelatin, thus hindering the drug adsorption [43].

Several literature sources dealing with the impregnation of spherical vaterite particles of different sizes with PDT drugs also confirm that the small particle size is not a distinct parameter responsible for high loading. For instance, the LC of vaterite particles with Photosens was 1.4 ± 0.4 wt% and 0.9 ± 0.2 wt% for the particles with a diameter of 0.7 μm and 3.6 μm, respectively [34]. However, in the case of Photoditazin, the reported corresponding LC values were 3.2 ± 0.6 wt% and 3.0 ± 0.5 wt% for the particles with an average diameter of 0.5 μm and 5.0 μm, respectively [44]. To reach the average loading of Photoditazin above 3 wt%, the authors had to optimize the photosensitizer concentration in the applied dye solution [44].

2.1.2. Molecular weight and net charge of payload

Zeta-potential of $CaCO_3$ vaterite microparticles synthesized via the classical route (i.e., by mixing aqueous solutions of $CaCl_2$ and Na_2CO_3 taken in equal molar concentrations) is usually about zero varying from weakly positive, e.g., ~+5 mV [45], to weakly negative, e.g., ~-14 mV [46]. The opposite net charge of the payload with respect to vaterite was found to be beneficial for catalase, insulin, protamine, aprotinin [45], bovine serum albumin [47], lysozyme [48], and doxorubicin [49].

Catalase and insulin that are negatively charged at physiological pH were loaded in weakly positively charged vaterite in relatively high amounts. By contrast, positively charged protamine and aprotinin didn't get adsorbed that well and did get quickly released from vaterite particles upon washing. Overall, catalase and insulin had the loading of 0.034 wt% and 0.023 wt%, respectively, which was an order of magnitude greater than the loading of positively charged protamine and aprotinin (0.0034 wt% and 0.0011 wt%). Confocal microscopy studies revealed that catalase and insulin were distributed evenly across the whole volume of the vaterite microspheres, indicating no limitations on diffusion through the vaterite mesoporous structure [45]. Unrestricted diffusion was favored because the dimensions of the microsphere pores (20–60 nm) were larger than the hydrodynamic diameters of the proteins (15 nm for catalase and about 4 nm for other proteins studied) [45].

Further studies of the vaterite loading with catalase (250 kDa), insulin (5.8 kDa), and aprotinin (6.5 kDa) unexpectedly revealed no direct correlation of LC with the protein's molecular weight and net charge. The largest protein, catalase, exhibited easy penetration into the particle pores; however, charge and/or steric limitations restricted the diffusion of the much smaller insulin and aprotinin [50]. The root cause seems to be an inter-protein aggregation mediated by Ca^{2+}, which occurred either in the bulk phase (for aprotinin) or on the crystal surface (for insulin). Aggregation of aprotinin in the bulk phase prohibited its loading into the carbonate cavities. The authors believed that the formation of insulin hexamers in the bulk phase initially promoted their diffusion into the particle pores. However, the penetrating hexamers would then aggregate inside the pores, thus blocking the additional insulin hexamers from diffusing inward. The catalase molecules didn't form aggregates in the presence of $CaCO_3$, and thus, according to the author's opinion, they only had sterical restrictions upon diffusion into the smallest pores of vaterite [50].

2.1.3. Payload concentration in solution

The concentration of payload substance in the solution used for the adsorption process is one of the crucial parameters that ultimately affect the LC of the method. It heavily depends on the solubility of the payload substance in the selected solvent or solvent system. Quite often, when the adsorbed payload is valuable and best not to be wasted, LC can be deliberately decreased in favor of higher LE by increasing the number of vaterite particles used for loading.

In this regard, raising the concentration of PDT drug, photodiazine, to 2.5 mg/ml as a result of an optimization approach yielded almost equal LC (3.2 wt % and 3.0 wt %) for vaterite particles of substantially different sizes, 500 nm, and 5 μm, respectively [44]. An increase of the doxorubicin concentration from 1 g/L to 6 g/L led to a rise in LC from 3 ± 2 wt% to 11 ± 3 wt% [49]. A high loading of vaterite with doxorubicin observed in that study was interpreted as an outcome of electrostatic interactions between the oppositely charged microparticles and payload.

Adsorption of macromolecules generally follows the same trend. For instance, alkaline phosphatase immobilization on vaterite with particle size 1.15 ± 0.07 μm produced a slightly higher LC upon increasing the enzyme concentration from 1 g/L to 10 g/L [37]. The loading data were measured directly upon the dissolution of $CaCO_3$.

2.2. Loading of a single drug

Various proteins of different origin and molecular weight, for example, catalase [31,45,50], protamine [45], DQ–ovalbumin [51], lactoferrin [52], cortexin [53], were successfully loaded into vaterite. In Ref. [54], CaCO3 microparticles were impregnated with low (betamethasone) and high (erythropoietin) molecular weight hormones. This study further reports sustained release of the incorporated drugs both *in vitro* and *in vivo*.

Numerous publications describe encapsulation of drugs with anticancer activity, e.g. cisplatin [27], doxorubicin [24,42,44], etoposide [56], Photosens [57], etc. In general, these accounts report an enhanced bioeffect as a result of the successful incorporation of the drugs in the $CaCO_3$ carriers.

Wang et al. [29] encapsulated a low molecular weight NSAID drug ibuprofen via diffusion into the vaterite pores. The authors demonstrated a faster release of ibuprofen in the gastric fluid and a slower release in the intestinal fluid compared to the ibuprofen alone. Low molecular weight antifungal drugs, griseofulvin, and naftifine, were respectively loaded in $CaCO_3$ [58,59] using co-precipitation (for griseofulvin) and both co-precipitation and adsorption methods for naftifine. Comparative spectrofluorimetric data indicated a higher naftifine loading (9 wt%) after co-precipitation [59]. Naftifine-loaded submicron $CaCO_3$ particles were effectively internalized by NHDF cells increasing the drug bioavailability *in vitro* through a prolonged release [60].

2.3. Concomitant loading of multiple drugs

One of the many attractive features of $CaCO_3$ vaterite is the possibility of simultaneous delivery of multiple drugs that may provide an improved efficacy assigned to a possible synergistic effect of active compounds. Such “molecular cocktails” can be

encapsulated by means of either of the two loading methods. However, the loading efficiency of each particular cocktail component can vary significantly compared to its individual loading due to the adsorption competition between the cocktail molecules as a result of their different affinity to $CaCO_3$, spatial restrictions, diffusion limitations, ionic interactions, etc.

A typical example is the loading of multiple chemotherapeutic drugs in submicron-sized vaterite particles performed by Cheng and coworkers [28,61,62]. In a most typical approach [28], paclitaxel and doxorubicin (as doxorubicin hydrochloride) were sequentially encapsulated in <200 nm sodium alginate pre-loaded porous $CaCO_3$. Paclitaxel from its acetone solution was loaded first, followed by evaporation of solvent and loading particles with doxorubicin in water. The protocol yielded vaterite particles containing 0.09 wt% of paclitaxel and 0.01 wt% of doxorubicin. For comparison, the same conditions applied for a single drug loading provided 0.09 wt% of paclitaxel and 0.04 wt% of doxorubicin. A lower amount of encapsulated doxorubicin upon the sequential loading is obviously due to the decreased pore volume by priorly loaded paclitaxel.

Cheng's group later developed a co-precipitation loading method, which involved doxorubicin hydrochloride, heparin sodium salt, protamine sulfate, and tariquidar and achieved the following LCs for doxorubicin in two different compositions: heparin/protamine sulfate/$CaCO_3$/doxorubicin − 9.5 wt%, heparin/protamine sulfate/$CaCO_3$/doxorubicin/tariquidar − 7.9 wt% [53]. It is worth mentioning that the LE of doxorubicin in the tariquidar-containing process was also lower than that without tariquidar, i.e., 80% vs. 96.3%. However, the presence of tariquidar in a cocktail of doxorubicin and carboxymethyl chitosan or biotinylated carboxymethyl chitosan didn't affect the drug loading in a similar co-precipitation process. The obtained LCs were 1.37−1.38 wt% and 1.40−1.42 wt% with and without tariquidar, respectively [61].

2.4. Methods to increase the loading capacity

Aside from the earlier, generally known ways to increase the particle LC, e.g., allowing more adsorption time until the process is equilibrated [37], a few novel approaches have emerged in recent years, with particular attention paid to the improved loading of low molecular weight compounds and preventing their premature release.

2.4.1. Adding adjuvants

Adding various large-sized molecule adjuvants, e.g. biopolymers or synthetic polymers, to $CaCO_3$ vaterite microcrystals is considered as a direct approach to increasing the loading of water-soluble compounds and to the slower subsequent cargo release, which often involves an electrostatic interaction between the adjuvant molecules and the payload. For instance, adding dextran sulfate to vaterite particles led to a higher absolute value of their ζ-potential that resulted in 5−10 times increase of peptide loading [63], wherein the particles with adsorbed dextran sulfate showed ca. two times higher LC than those obtained by co-precipitation.

Lysozyme binding to heparin was used to load the protein into heparin-containing vaterite crystals and retain it with good efficacy during the consequent layer-by-layer coating [48]. However, despite the presence of heparin, the co-precipitation method had a very limited ability to load lysozyme. A reasonable LC of 0.0916 wt% was achieved by post-loading the protein into heparin-pre-loaded $CaCO_3$ in water after a short ultra-sonication treatment. Most importantly, the activity of the encapsulated lysozyme was almost fully retained.

Siloxane-modified vaterite particles had a positive zeta potential of +44 mV that assisted in absorbance of 0.04 wt% of negatively charged bovine serum albumin [47]. However, the particle loading with positively charged lysozyme was also apparent (0.014 wt%), indicating that electrostatic interactions may not be a predominant factor in the reported case. In another prominent study, Osada et al. [47] studied the protein content in siloxane-pre-loaded and pure $CaCO_3$ depending on the adsorption time. The highest loading of BSA was observed after two days of incubation of the $CaCO_3$ particles in protein solution for both particle types. Further increasing of the adsorption time did not influence the protein content for the siloxane-modified vaterite. Pristine vaterite contained no BSA even after the eight days of adsorption. This result is explained by the gradual recrystallization of vaterite particles into the non-porous calcite. Unlike BSA, both siloxane-modified and pure vaterite particles displayed the highest lysozyme content after two days and no trend of decreasing the amount of protein upon extended incubation, indicating the lysozyme's tendency to impede recrystallization of $CaCO_3$.

Interestingly, the use of BSA (at 15 wt%) as an adjuvant did assist in the facile preparation of porous $CaCO_3$ vaterite crystals that improved their stability in water for 48 h. These particles were successfully loaded with the anticancer drug camptothecin using the adsorption approach. The resulting camptothecin-containing $CaCO_3$-BSA vaterite microcrystals had a well-defined drug release profile at lower pH (4−6, i.e., pH levels found in lysosomes and solid tumor tissues, respectively) while remained almost intact at neutral pH (7.4), typical for normal physiological conditions. Subsequent *in vitro* experiments demonstrated a sustained cell growth inhibitory activity for camptothecin-loaded vaterite particles pre-loaded with BSA [26].

Numerous examples of doxorubicin loading in $CaCO_3$ include the use of vaterite microparticles modified with carboxymethyl cellulose (LC = 0.475 wt%) [64], carboxymethyl chitosan (LC = 1.4 wt%) [28], and gelatin (up to 0.03 wt%) [55]. Besides higher loading, oppositely charged molecule adjuvants (e.g., gelatin) reportedly resulted in a slower doxorubicin release, enhancing the drug's bioeffect *in vitro* [67].

Gao's group studied doxorubicin hydrochloride loading in carboxymethyl cellulose-modified 5 μm particles of $CaCO_3$, reporting a significant decrease in specific surface area, total pore volume, and a change in the pore size distribution of the vaterite after the drug adsorption [64]. Using the Brunauer−Emmett−Teller method, the authors presumed that doxorubicin molecules predominantly occupied pores and accumulated on the surface of microparticles reaching the LC of 0.475 wt%. After the drug loading, the volume of small pores decreased significantly while the volume of larger ones slightly increased. The increase in the larger pores' volume was explained by electrostatic interactions between carboxymethyl cellulose and doxorubicin, resulting in a more spatially compact complex [64].

This manuscript represents well-documented research with a number of interesting observations. Yet, it is essential to note that the reported results were obtained using the methods developed for water-soluble substances and drugs involved in the assembly of such complex particles. Doxorubicin, however, is only soluble in aqueous solutions in the salt form (as the hydrochloride in this case) among the studied drugs. In the molecular surrounding where there is a number of other salts capable of neutralizing the hydrochloride (and thus precipitating doxorubicin from aqueous medium), it is quite hard to predict if indeed the reported very high LC is achieved by precipitation caused by chemical neutralization or by electrostatic interaction explained by the authors.

Bosio et al. [68] performed comprehensive research on the capacity of different biopolymers to increase doxorubicin loading in vaterite. In the first step, thirteen biopolymers, including three carrageenans, three chitosans, hyaluronic acid, five pectins, and xylan, were screened as potential matrices for doxorubicin loading. λ-, κ-, and ι-carrageenans showing the strongest affinity to doxorubicin were taken to the next stage, i.e., vaterite synthesis and loading. The range was further narrowed down to λ-carrageenan as providing vaterite particles with the smallest polydispersity in respect to the size and shape. The authors also optimized the doxorubicin adsorption conditions for the obtained modified microcrystals to maximize loading. The best conditions found, providing LE = 29 %, were pH 6.5 with MES buffer under slow stirring at 4 °C for 6 h. For comparison, the authors [68] had reported that the same protocol of loading doxorubicin in pure vaterite microparticles gave LE close to 0%. Chemical derivatization of λ-carrageenan with folic acid primarily aimed at tumor-targeting further increased LE to 83%. Bosio et al. explained such a significant difference in the loading by the increased number of carboxylate groups formed due to the attachment of folic acid to carrageenan and due to the hydrophilicity of doxorubicin [68]. However, as noted above for the results of Gao et al. [64], it is expected that the hydrophilicity and, respectively, the solubility of doxorubicin in aqueous media will drop dramatically if doxorubicin hydrochloride salt can get neutralized during its attempted loading. Once the insoluble free base of doxorubicin is formed and precipitated from the solution, the typically used residual UV determination method, i.e., measurement of the remaining concentration of doxorubicin hydrochloride in the supernatant (e.g., in Ref. [64]), would expectingly result in artificially higher values: while only a negligible amount of water-soluble doxorubicin hydrochloride salt is still present, the bulk of doxorubicin is in the free base (i.e., insoluble) form, even if it is not encapsulated or entrapped in the particles. As a result, such residual UV determination would give incorrect, elevated values of "loaded" doxorubicin. For more accurate measurements, using DMSO instead of water-based solutions is preferred (see example [69]).

The binding capacity of mucin, forming hydrogen bonds and capable of electrostatic and hydrophobic interactions with various therapeutics is often exploited to improve loading in vaterite-based delivery systems. Balabushevich and coworkers used mucin in the synthesis of $CaCO_3$ to increase the post-loading of doxorubicin [70] and aprotinin [13,70]. Mucin adding resulted in an increase of doxorubicin and aprotinin contents in vaterite particles by a factor of twelve and three, respectively. The release of the drugs from such mucin-pre-loaded microcrystals was almost twice lower than from mucin-free counterparts, supporting the idea of strong binding between the active compounds and adjuvant [70].

Besides soluble biopolymers discussed above, self-assembled complexes (e.g., micelles) can also be successfully applied as adjuvants for vaterite.

Ying et al. [66] reported a significantly higher doxorubicin loading via co-precipitation with starch-octanoic acid micelles than a starch on its own. In another work, vaterite microspheres co-precipitated with casein micelles for better morphological stability, and cyclodextrins for higher porosity, were used as a delivery system for post-loaded minocycline [71]. In this case, the adjuvant agents, cyclodextrins, were responsible for a larger surface area and, accordingly, more mesoporous vaterite structure, yielding a higher drug loading than cyclodextrins-free microparticles.

Another way to increase the vaterite loading is by using additives, such as polyethylene glycol, during vaterite synthesis. Singh and Sen [72] studied co-precipitation of $CaCO_3$ with an antibacterial drug, sulphanilamide, performed in ethanol/water/polyethylene glycol mixture. The process yielded a 3-4-fold increase in drug loading compared to co-precipitation in ethanol/water mixture alone. The authors presumed that the molecular mobility was restricted in a viscous PEG solution, which facilitated preferential interaction between sulphanilamide and $CaCO_3$ and more efficient drug entrapment in the porous matrix.

Functionalization of the vaterite surface with silanes increased the surface hydrophobicity, which is believed to facilitate a better cisplatin loading and retention [73]. According to the authors, such modification allowed to achieve 23.9×10^{-5} wt% of cisplatin content for silane-containing vaterite compared to 15.8×10^{-5} wt% of the pure vaterite loaded drug.

A useful tool for direct loading of vaterite microparticles, adjuvants can also facilitate a spontaneous payload absorption by polymeric multilayer capsules formed on the modified cores, thus, increasing their LC. For instance, this technique was applied to load a growth factor, TGF-b1, into hollow microcapsules assembled on heparin-containing $CaCO_3$ [64].

2.4.2. Solvent evaporation in a vacuum and centrifugation

Sudareva et al. [63] did compare LCs of $CaCO_3$ microparticles with lysozyme and neuroprotective peptides of different molecular weights and isoelectric points using four loading methods: co-precipitation, adsorption on pre-formed cores, "exhausting vacuumization" (this definition, which is given in the original manuscript, actually means complete evaporation of the solvent(s) in the vacuum chamber; for clarity, in this review, it will be changed to "solvent evaporation in a vacuum"), and adsorption combined with centrifugation.

The reported conditions essential for a fair comparison between the loading methods were as follows: 1. *Co-precipitation:* the active compound that was initially dissolved at 0.4–0.6 mg/mL was added to 3 mL of 0.33 M $CaCl_2$; this solution was then mixed with the equal amount of Na_2CO_3 (0.33 M), followed by particle washing (all compounds were dissolved in water); 2. *Adsorption:* $CaCO_3$ core suspension prepared in a peptide or lysozyme solution of 0.4–0.6 mg/mL was incubated for 90 min followed by particle washing; 3. *Solvent evaporation in a vacuum:* $CaCO_3$ core suspension prepared in a peptide solution (3–7 mg/mL) was placed into a vacuum chamber with a residual pressure of 30 mm Hg for 20 h until complete evaporation of the solvent; 4. *Adsorption combined with centrifugation:* $CaCO_3$ core suspension prepared in a peptide or lysozyme solution (0.4–0.6 mg/mL) was centrifuged at 8000 rpm for 30 min, followed by particle washing. The authors concluded that compared to the classical adsorption method, where the concentration gradient exclusively drives molecule diffusion, the studied combination of adsorption with centrifugation creates an additional effect (based on centripetal force) that favors a higher loading.

Comparative loading data obtained by each method are given in Table 1. Interestingly, the size restriction plays a different role in the methods studied. The standard co-precipitation does not allow for high LCs with the studied compounds except for a large molecular weight lysozyme, which was likely to get stuck in the pores upon the particle washing – per authors, this was detected more readily than for the peptides that have the smaller molecular weights. The adsorption method provided better loading for the peptides but was not efficient for lysozyme, apparently because of its larger molecule size restricting its diffusion deep into the pores of $CaCO_3$.

Among the compounds loaded by either adsorption or centrifugation method, the particle loading using centrifugation was remarkably beneficial for U5, a peptide with the lowest molecular weight and the highest pI (0.89 kDa, pI 9.8): 74 ± 10 wt% upon loading by the centrifugation method vs. 9 ± 10 wt% by the adsorption. Lysozyme, having the largest molecular weight and the highest pI (14 kDa, pI 11.0), was also loaded more efficiently with

Table 1
Loading of peptides into $CaCO_3$ particles using different procedures: LC, 10^{-3} wt% (Reproduced from Ref. [63]).

Payload	Loading procedure			
	Co-precipitation	Adsorption from H_2O (diffusion), 90 min	Solvent evaporation in a vacuum before (bw) and after (aw) washing	Centrifugation (30 min at 8000 rpm)
				in H2O **in 0.15M NaCl**
U2 1.66 kDa, pI 9.0	9 ± 3	18 ± 2	38 ± 5 bw 23 ± 4 aw	20 ± 6 8 ± 6
U5 0.89 kDa, pI 9.8	1 ± 2	9 ± 10	21 ± 5 bw 18 ± 3 aw	74 ± 10 16 ± 5
U7 1.26 kDa, pI 9.4	4 ± 2	–	50 ± 6 bw 12 ± 3 aw	11 ± 3 –
B7 0.99 kDa, pI 6.6	3 ± 1	7 ± 2	32 ± 5 bw 0 aw	10 ± 3 0
Lysozyme 14 kDa, pI 11.0	25 ± 5	8 ± 2	–	54 ± 4 0

centrifugation: 8 ± 2 wt% vs. 54 ± 4 wt% in the adsorption and centrifugation method, correspondingly. The respective data for U2 (1.66 kDa, pI 9.0) and B7 (0.99 kDa, pI 6.6) loading were similar in both methods within the experimental error.

To prove that the loading of $CaCO_3$ microparticles using the combined adsorption/centrifugation technique is driven by the infliction of electrostatic interactions and centripetal force, the authors exchanged the water medium for 0.15 M NaCl. As a result, the respective loading drastically decreased for all studied compounds.

The solvent evaporation in a vacuum approach gave the highest LCs for each peptide (measured after the solvent evaporation) when compared with other loading methods. However, consecutive particle washing did remove loosely residing molecules, which resulted in a considerable loss of the payload; the LC was comparable to the one obtained after molecular adsorption within the experimental error. As it appears, to achieve high efficiency, the solvent evaporation in a vacuum method requires very high peptide concentrations and also takes about 20 h to be completed. Not only are these conditions destructive for peptides, but they can also lead to recrystallization of vaterite into calcite. Therefore, this method has to be applied with care, considering the stability of the payload and the possibility of vaterite recrystallization [48,54].

2.4.3. Freezing

German et al. [20,76] recently introduced freezing as a novel approach to increase the loading of molecules and nanoparticles in vaterite crystals. The method showed higher efficacy than either adsorption or co-precipitation. Moreover, the process can be repeated to increase the loading content even further. The loading routine involves successive cycles of freezing and thawing a suspension of porous particles in a drug solution or a suspension. Freezing results in all dispersed objects being pushed by the crystallization front during solvent crystallization so that the loaded species first concentrate over the interface of the vaterite particles and then embedded in pores and surface of the $CaCO_3$ particles by the growing pressure of the forming solvent crystals. Such embedding of the payload into vaterite is probably a common feature of the freezing and combined centrifugation methods.

Critical for this method's successful application is the possibility of precisely controlling the end of the freezing process [74]. German et al. developed a device for remote *in situ* monitoring of the liquid crystallization to provide the technologically most essential parameters, such as the ice/water interface velocity in water colloids/suspensions and the moment of the final adsorption of the nanoparticles on the microparticles. In the setup, the system is followed via Raman spectroscopy by directly observing the hydrogen bond formation during crystallization and the sorption of nanoparticles.

The freezing-induced approach applied for the micron-sized $CaCO_3$ loading provided more than a three-times higher loading for magnetite nanoparticles and a four-times higher loading for a protein such as BSA compared to adsorption co-precipitation methods (Table 2) [20]. Essentially, the freezing-induced adsorption of magnetite in vaterite allowed to reach a very impressive LC of 42 wt% [75].

Besides magnetite and BSA [31,62], the method was successfully applied to impregnate vaterite with Au [20] and TiO_2 [21] nanoparticles. Remarkably, the loading of TiO_2 nanoparticles in vaterite through adsorption at ambient conditions failed due to electrostatic repulsion. Freezing the suspension of $CaCO_3$ and TiO_2 resulted in a sufficient loading to ensure the photocatalytic activity of polyelectrolyte capsules templated on the obtained TiO_2—$CaCO_3$ [21]. In Ref. [77], the authors developed hybrid mineral highly-magnetic protein—tannin vehicles with encapsulated anticancer drugs, demonstrating the maximum saturation of calcium carbonate submicron particles by the freezing-induced loading technique.

3. Drug delivery *in vivo*

Numerous research publications describe efficient *in vitro* delivery of drugs by $CaCO_3$ micro- and nanosized particles, highlighting the benefits of vaterite as a delivery vector. The representative examples of successful *in vitro* application of vaterite include refs. [10,43,56,57,65,66]. On the other hand, the amount of articles dedicated to *in vivo* studies of vaterite-assisted drug delivery is much fewer but continuously increases every year. This chapter provides a detailed overview of the most recent advances in porous $CaCO_3$ particle applications for *in vivo* delivery of therapeutics *via* injections and other parenteral and oral administration routes.

3.1. Injection administration routes

3.1.1. Intravenous injections

One of the early prominent works describing *in vivo* application of the pristine $CaCO_3$ for anticancer therapy in rodents was published in 2016 by Som et al. [78]. The authors reported selective accumulation of nanosized $CaCO_3$ (20—300 nm) in murine models of cancer, leading to increased tumor pH over time, which allowed for the alleviation of tumor acidosis. In this pioneering work, the nanosized $CaCO_3$ particles showed the ability to localize selectively in the extracellular region of tumors, increasing and maintaining tumor pH at ~7.4 due to high buffering capacity (Fig. 1). The

Table 2
Comparison of loading content of different substances into vaterite particles [20].

Loaded substance	Freezing-induced loading, LC wt.%	Adsorption, LC wt.%	Coprecipitation, LC wt.%
Fe_3O_4 magnetite nanoparticles	13	4	3
BSA	13.5	3.7	3.6

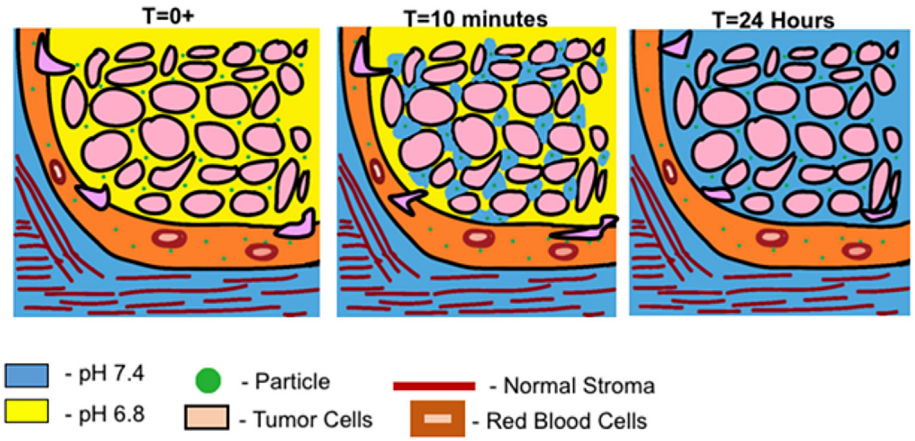

Fig. 1. Dynamic representation of nano-$CaCO_3$ effect: a high dose of $CaCO_3$ enters tumor tissue via enhanced permeation and retention (EPR) effect and increases pH to 7.4. Over time this continuous dose allows for continuing maintenance of pH 7.4. Reprinted with permission from Ref. [78]. *Copyright* © 2015, The Royal Society of Chemistry.

vaterite-induced pH changes, as a result, hindered or reduced cancer progression.

In the subsequent study, Som and coworkers [79] confirmed the biocompatibility and negligible toxic effect of the vaterite nanoparticles *in vitro* and *in vivo*. The researchers also presented a noninvasive biodistribution study of magnetite-doped nanosized $CaCO_3$ particles using magnetic resonance imaging (MRI) and positron emission tomography (PET) in two types of solid tumors. Accumulation of magnetite-$CaCO_3$ particles in fibrosarcoma tumor after intravenous injection of HT1080 tumor-bearing mice caused a decrease in T2 relaxation time (increase in R2), consequently appearing in the kidney and liver and finally in the tumor (Fig. 2a). The T2 signal throughout the animal body decreased rapidly with a trough at around 6 h, followed by the return of signal approaching the original T2 profile at the 24 h time point (Fig. 2b). The significant reduction of T2 in the bladder suggested a substantial renal clearance component, whereas T2 recovery in the tumor indicated that the magnetite-$CaCO_3$ was dissolving in the tumor's acidic pH as designed, and the free magnetite was clearing from the tissue. It was also discovered that the administration of nano-$CaCO_3$ could cause reprogramming of metabolic function of tumors: $CaCO_3$ injected into a tail vein of HT1080 fibrosarcoma-bearing mice reduced the glucose analog uptake in the tumor by a statistically significant margin with no changes of that in muscles (Fig. 2c).

$CaCO_3$ nanoparticle accumulation induced a transient pH increase in the tumor microenvironment in the breast cancer model followed by an overcompensation of acidity by the tumor upon nanoparticle clearance in 24 h as a metabolic reprogramming response of the cancer cells to extracellular pH change (Fig. 2d). Additionally, continuous infusion of nanosized $CaCO_3$ did inhibit the tumor metastasis in the model of aggressively metastasizing 4T1luc-GFP orthotopic breast cancer [79].

Svenskaya et al. [35] studied the effect of vaterite particles as a delivery system for a photodynamic therapy drug, Photosens. Loaded vaterite particles were intratumorally injected in the PC1 strain alveolar liver cancer that was hypodermically implanted into the rat scapular area. The authors utilized an ultrasound-induced (5 min, 0.89 MHz, 1 W/cm^2) destruction and concomitant recrystallization of vaterite into calcite polymorph for the drug release in combination with the light irradiation (670 nm, 10 mW/cm^2) for reactive oxygen species generation. Compared with the unloaded vaterite, the Photosens-bearing particles promoted distinct dystrophic changes in tumor cells and the origination of extensive necrotic centers [35].

The tumor-specific accumulation and pH-sensitive properties of $CaCO_3$ nanoparticles were used by Kim et al. [80] to target lung cancer cells with the intracellular-acting therapeutic peptide, EEEEpYFELV. The peptide-loaded particles were coated with cationic lipids and conjugated with anisamide, a ligand that targets the sigma receptor expressed on lung cancer cells. The obtained formulation mediated specific delivery of the peptide to tumor tissue after intravenous injection to the NCI—H460 xenograft tumor-bearing mice, suppressing the tumor growth three times more efficiently than a peptide alone. Additionally, the nanoparticle-enhanced anticancer activity was attributed to the pH-controlled release due to the dissolution of $CaCO_3$ in the endosomes, which are acidic. The applied formulation showed minimal uptake by external organs and did not express any toxicity [80].

Due to the relatively small size, doxorubicin molecules are rapidly excreted from the bloodstream by glomerular filtration in kidneys, making it difficult to maintain the drug concentration at the therapeutic level over time. Intending to extend the systemic presence of doxorubicin, Zhang et al. [81] conducted an impressively detailed study of *in vivo* stability, biodistribution, and the efficacy of tumor inhibition to discover the potential of vaterite particles for cancer treatment using hyaluronic acid/doxorubicin-loaded vaterite nanoparticles (HA-DOX/$CaCO_3$), free doxorubicin (DOX), and its complex with hyaluronic acid (HA-DOX). The authors explained the observed efficacy of HA-DOX/$CaCO_3$ nanoparticles by the apparent electrostatic bonding of DOX to hyaluronic acid in $CaCO_3$ [81]. Unfortunately, even though the supplementary section of the manuscript does provide a synthetic protocol, it still lacks clarity of how the HA-DOX/$CaCO_3$ particles were assembled. Unlike

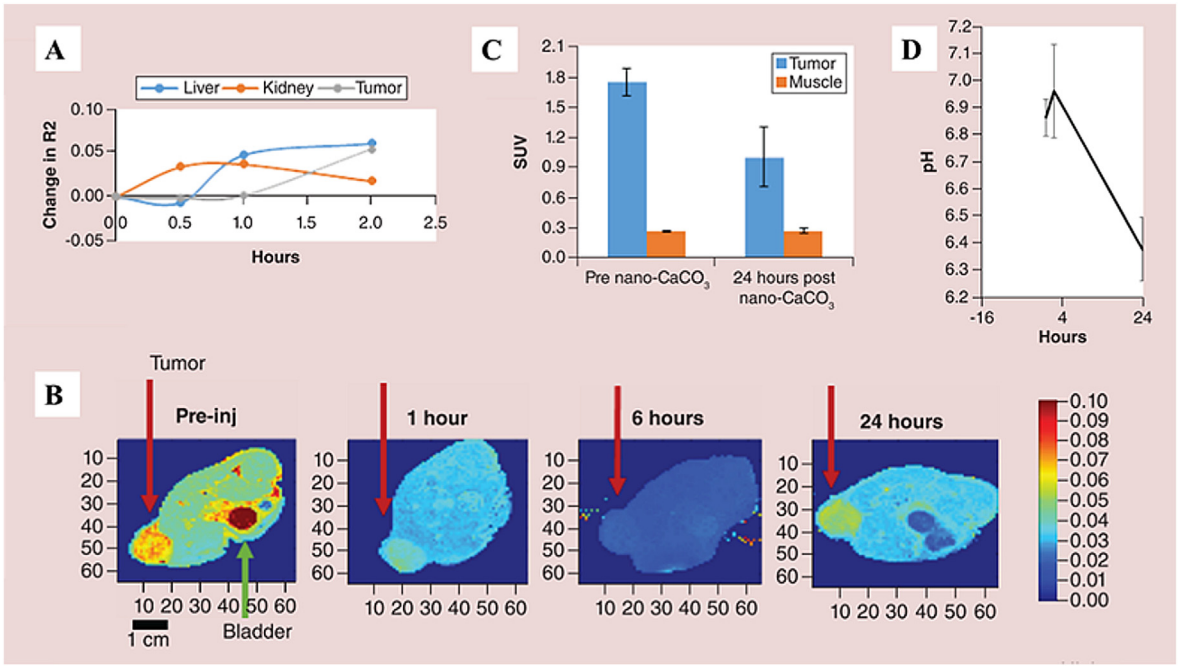

Fig. 2. (A) Change in R2 (1/T2) over time in the liver, kidney and HT1080 tumor after injection of magnetite-$CaCO_3$. (B) Visualization of T2 changes with magnetite-$CaCO_3$ injection in a cross-section of a mouse (representative images of n = 3 mice). Red arrow shows tumor, green arrow shows the mouse's bladder. Note the drop in T2 throughout, with recovery by 24 h. Heat map shows relative T2, with red and blue indicating high and low activity, respectively. (C) Tumor versus muscle uptake of glucose analog 18F-Fluorodeoxyglucose (FDG) after HT1080 tumor-bearing mice were given a tail vein injection of $CaCO_3$ nanoparticles (n = 3 mice). (D) MRI-based tumor pH measurement in a breast cancer MDA MB-231 model treated with $CaCO_3$ nanoparticle (n = 3 mice, one experiment). Adapted with permission from Ref. [79]. *Copyright* © 2018, Future Medicine Ltd.

it is explained in the manuscript, it is expected that in the first step, i.e., the reaction of a large excess of HA with DOX (both were used in the form of sodium salt for HA and of hydrochloride salt for DOX), a mixture of DOX free base and HA as partially neutralized free acid is formed. Such mixture should not form a complex based on electrostatic interaction as both species were not ionized in water. In the next step, reaction of HA with calcium nitrate hexahydrate was performed. An important feature of such interaction is that the neutralization of COOH groups of HA by calcium cations will be done evenly, not only in the specific area of HA macromolecules, i.e. it will not form a relatively dense core, per drawing provided in the paper, but rather would form a relatively loose network of HA with two-valent calcium cations, based on the ratio of HA to calcium nitrate. Addition of sodium carbonate would precipitate $CaCO_3$, but again this would not be a "core"-like formation but an evenly spread nuclei of $CaCO_3$ stretched across HA polymer network containing the previously made mixture of HA with DOX. Overall, the particles obtained in the cited manuscript would not be represented by suggested dense $CaCO_3$ core with protruding and extending side chains of HA carrying DOX, which was attached as a result of electrostatic interactions, but rather would appear as uniform mesh-like particles, where long polymeric chains of HA together with neutralized DOX molecules are trapped within $CaCO_3$ crystals.

One additional issue with the use of HA in conjunction not only with $CaCO_3$ but with any other delivery system is the abundance of hyaluronidases, the enzymes responsible for cleavage of hyaluronans found in most of the tissues, e.g., HYAL1 and HYAL2. There are at least five hyaluronidases in humans, and their action would affect the use of HA in the studied particles. This possibility was not addressed in the paper.

Nonetheless, the overall results of the cited manuscript seem to provide valuable information related to *in vitro/in vivo* applications of such particles. As shown in Fig. 3a, HA-DOX/$CaCO_3$ particles had a longer blood circulation time than DOX and HA-DOX with respective half-life periods of 10.4 h, 15.1 h, and 23.5 h for DOX, DOX-HA, and DOX-HA/$CaCO_3$.

A biodistribution study in K7 osteosarcoma-allografted BALB/c mice six or 12 h after the administration revealed similar accumulation levels among the studied drug forms by heart, spleen, lung, and kidney and a slightly elevated accumulation of the encapsulated drug in the liver at the 12 h time point. The target tumor tissue, however, displayed a significantly higher level of doxorubicin for the group of mice injected with HA-DOX/$CaCO_3$ than for the other groups at 6 h ($P < 0.001$) and 12 h ($P < 0.05$) post-injection (Fig. 3b), wherein the lowest level of the drug in the tumor tissue was in mice treated with DOX. Twelve hours after administration, the fluorescence signal from doxorubicin located in the mice tumor tissue that received the drug in the encapsulated form was 2.6 and 1.3 times higher than that in the control groups injected with DOX and HA-DOX, respectively.

In agreement with the biodistribution study, calcium carbonate nanoparticles loaded with doxorubicin successfully inhibited tumor growth in K7 osteosarcoma-allografted mice with an initial tumor volume of 200 mm^3 (Fig. 4a) [81]. A group of mice injected with HA-DOX/$CaCO_3$ was compared with two control groups treated with DOX and HA-DOX, respectively, to reveal the drug encapsulation benefits. After four days of therapy, the experimental group demonstrated the most efficient cancer suppression, inhibiting tumor growth by 84.6% (Fig. 4b and c). On average, the effect of encapsulated drug form was 2.2 and 1.3 times better than that of the DOX group (39.0%) and the HA-DOX group (62.9%). The HA-DOX/$CaCO_3$ drug form also showed higher anticancer activity than two other studied counterparts in the primary model of murine osteosarcoma.

Systemic toxicity of doxorubicin is another issue that could be resolved by encapsulation in vaterite. In the experiments performed by Zhang et al. [81], the tumor-bearing mice in the HA-

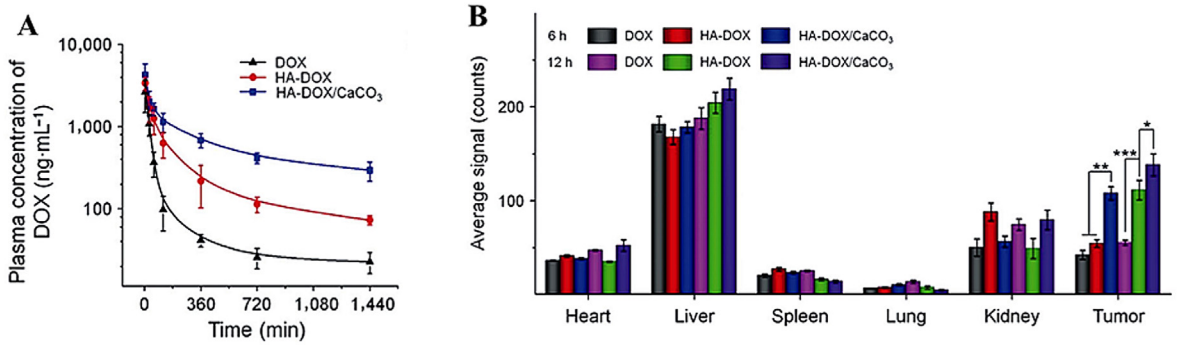

Fig. 3. (A) *In vivo* pharmacokinetic profiles of free DOX, HA-DOX, and HA-DOX/$CaCO_3$ in mice. (B) Average signals of tumors and organs at 6 or 12 h post-injection of free DOX, HA-DOX, or HA-DOX/$CaCO_3$ into K7 osteosarcoma-allografted BALB/c mice. The statistical data are presented as mean ± standard deviation (n = 3; *P < 0.05, **P < 0.01, ***P < 0.001). Adapted with permission from Ref. [81]. *Copyright* © 2018, SpringerNature.

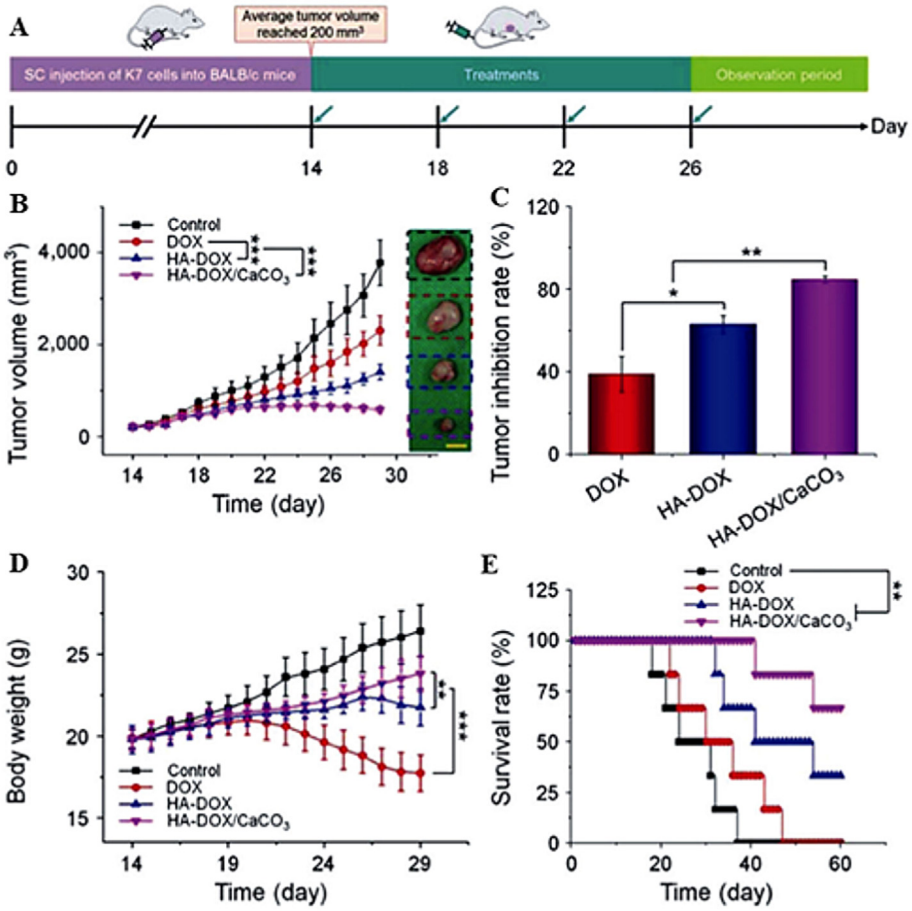

Fig. 4. *In vivo* antitumor efficacy in K7 osteosarcoma-allografted mice with an initial tumor volume of 200 mm^3. (a) Experimental schedule for tumor induction and drug treatments. (b) Tumor volumes, (c) tumor inhibition rates, (d) body weight changes, and (e) survival rates of mice treated with PBS as a control, free DOX, HA-DOX, or HA-DOX/CaCO3. Scale bar: 1.0 cm. The statistical data are presented as mean ± standard deviation (n = 8 for (b)–(d); and n = 6 for (e). *P < 0.05, **P < 0.01, ***P < 0.001). Adapted with permission from Ref. [81]. *Copyright* © 2018, SpringerNature.

DOX/$CaCO_3$ and HA-DOX treated groups showed no substantial body weight loss (Fig. 4d), indicating that no detectable toxicity of the respective drug forms was found. Besides, the survival time in groups treated with HA-DOX and HA-DOX/$CaCO_3$ was significantly longer than in the group receiving the free drug (Fig. 4e), while the longest survival time was observed in mice treated with the vaterite-loaded doxorubicin [81]. The stated enhanced chemotherapeutic efficacy of the HA-DOX/$CaCO_3$ drug form for treating both primary and advanced osteosarcomas at negligible signs of systemic toxicity is overall a reflection of successful tumor targeting by the vaterite particles with a spatially confined release of doxorubicin.

Song et al. [55] reported similar tumor-inhibiting activity of $CaCO_3$-loaded doxorubicin vs. free drug after intravenous injection into the H22 tumor-bearing mic, e.g., 64% vs. 37%, respectively. Noteworthy is that the vaterite particles used for drug

encapsulation in the cited paper had an average diameter of ~2 μm, indicating that the particle formulated drug in this size range still can outperform free doxorubicin even if the EPR effect is apparently not a major driving force.

Notwithstanding the delivery of chemotherapeutic drugs, vaterite nanoparticles were applied for building up a diagnostic probe in the intraoperative imaging of cancer cells to ensure their complete surgical excision [82]. The probe was composed of $CaCO_3$-embedded fluorescent molecules of Oregon Green derivative conjugated to a quencher chosen from cathepsin B substrates. The obtained particles of 200 nm in diameter were surface-modified with folate-PEG for tumor targeting. After administration via tail vein injection in MCF7 tumor-bearing mice, the particles accumulated at the tumor site followed by uptake with folate receptor and release of the molecular conjugate upon the vaterite dissolution under acidic pH in cancer cells. The quencher was then cleaved by cathepsin B so that the fluorescence was turned on under exciting light. A histology study indicated good biocompatibility of the particles with no visible pathological changes in the heart, liver, spleen, lung, and kidney one week after administration. This vaterite-based visualizing nanoprobe showed a high signal-to-noise ratio and precise and fast indication of tumor: in MCF7 tumor-bearing mice, the tumor was already visible 10 min after injection [82].

3.1.2. Intramuscular injections

A work of Sudareva et al. [83] highlighted the benefits of micron-sized vaterite for drug delivery via intramuscular injections, such as material safety and the microparticles' good potential for controlled drug release via undergoing recrystallization into a non-porous polymorph. Porous $CaCO_3$ microparticles with a diameter of 1–3 μm were transformed into needle-shaped crystals (30–150 μm long and 10–40 μm wide) in the muscle tissue one week after injection into the thigh great adductor muscles of hind extremities in rats. The modified particles, presumably aragonites, were then wholly erased by bioresorption in two weeks without negatively affecting the surrounding tissues. As a root cause of the recrystallization into aragonite, the authors proposed a few factors, including a slightly acidic shift of pH in muscle tissue, the reaction of carbonic acid formed in the metabolic process with $CaCO_3$, the action of immune cells, and mechanical impact related to muscle contraction [83]. Similar results were described in Ref. [84], where the porous spherical calcium carbonate vaterites were rearranged to form needle-like objects after three days of implantation with subsequent bioresorption during the following two weeks.

3.2. Other administration routes

3.2.1. Oral administration

Liu et al. [18] demonstrated an improved hypoglycemic effect in rats after oral administration of insulin-loaded vaterite particles compared with subcutaneous injection of insulin. The insulin-loaded nanosized vaterite (150–350 nm) coated with a folic acid-modified hyaluronic acid (FA-HA) layer exhibited low cytotoxicity against the HT-29 cells wherein encapsulation in vaterite effectively protected insulin from the loss of bioactivity. Per the authors' findings, after the oral administration of the insulin-loaded $CaCO_3$/FA-HA nanosized particles, the plasma insulin concentration increased at a low rate over the first 4 h and then slowly declined. Although the highest plasma insulin level upon oral administration of the vaterite-loaded insulin was less than after subcutaneous injection of the insulin solution alone, a higher plasma insulin level was maintained for a longer time in the case of oral delivery. More importantly, a slow release of insulin from the FA-HA-coated vaterite, as suggested by the authors, could potentially help to reduce the risk of hypoglycemia [18].

3.2.2. Intranasal administration

Several reports describe $CaCO_3$ as a useful carrier for intranasal delivery of insulin and hydrophilic compounds because of its ease of manufacturing and slow biodegradability. Haruta et al. [85] demonstrated intranasal delivery of the $CaCO_3$-loaded insulin in cynomolgus monkeys and healthy human volunteers. Four weeks after intranasal administration of the encapsulated drug in monkeys, the delivery system was found safe with no toxicity, even with a maximum insulin dose level of 25 U. Moreover, intranasally delivered vaterite-loaded insulin was absorbed much more rapidly than the insulin alone after subcutaneous administration. The former was also stimulating endogenous postprandial insulin secretion in healthy humans. The observed rapid and short-acting pharmacological effect against postprandial hyperglycemia suggests the vaterite-based particles for intranasal insulin delivery as a superior system to the existing pulmonary delivery formulations in the treatment of diabetes [85].

Ishikawa et al. [86] examined the absorption efficacy of model hydrophilic drugs with varied molecular weights that were administered to rats intranasally as a free form or as pre-formulated with "powders" (e.g., insoluble CaCO3, talc, BaSO4, ethylcellulose, or water-soluble mannitol, lactose, or sorbitol). The model compounds used were phenol red (MW = 354.38 g/mol), cyanocobalamin (MW = 1355.38 g/mol), and fluorescein isothiocyanate (FITC)-dextrans with an average molecular weight of 4400 Da, 9500 Da, 19,500 Da, 42,000 Da, and 77,000 Da. As a general trend, the systemic bioavailability of the studied compounds after intranasal delivery decreased with increasing the model drug molecular weights. CaCO3-based formulations of all studied compounds provided a significantly better absorption than the respective free model drugs and water-soluble "powder"-based drug forms. For the smallest compound tested, phenol red, the formulation with CaCO3 provided the same bioavailability upon intranasal administration as if a bolus dose was injected intravenously.

Microparticle-based therapeutic forms were explored by Bukreeva et al. [87] for loperamide intranasal delivery. The formalin test in rats was performed to assess the efficacy of loperamide delivery to the CNS by poly(butyl cyanoacrylate) nanoparticles, vaterite, and titanium dioxide microparticles. Among the particles studied, hyaluronic acid-coated CaCO3 microparticles (4 μm–6 μm) provided the most effective pain relief due to the enhanced CNS delivery.

Another interesting example of vaterite carriers' effective use in intranasal drug delivery was reported for a novel formulation of zolpidem (Ambien) [88]. Vaterite microparticles (3.5 μm ± 0.7 μm), preliminarily coated with a diethylaminoethyl-dextran/hyaluronic acid shell, were explored for nasal delivery of this anxiolytic drug in mice. The obtained zolpidem-loaded microparticles demonstrated a pronounced anxiolytic effect on animal behavior in the open field test, compared to the free drug efficacy upon intranasal delivery.

3.2.3. Pulmonary delivery

Delivery of therapeutics via inhalation is another administration route that was explored for vaterite-based drug formulations. Published data do provide sufficient evidence that a porous $CaCO_3$ may serve as an effective carrier to deliver drugs both locally to the respiratory portion of the lungs and systemically.

In the study by Gusliakova et al. [16], a model drug, BSA-Cy7, was packed in the vaterite of various particle sizes (0.65 μm, 1.35 μm, and 3.17 μm) followed by the particle administration to mice via tracheostomy. The research aimed to find the dependence

between the particle size and the loaded drug delivery efficacy and compare biodistribution between the encapsulated and free drug forms.

All studied particles showed the ability to penetrate the mouse lungs and deliver the payload systemically (Fig. 5). Compared to their larger counterparts, the submicron-sized particles showed a longer residing time in the lung (the delivered marker was well-seen 72 h after administration), the ability to reach the alveolar region, and the favorable pharmacokinetics for a slow release due to the reaction with the pulmonary surfactant components (Fig. 5). Both 1.35 μm and 3.17 μm particles were seen residing in the lung at the 24 h time point, but they almost entirely dissipated from the organ 72 h after administration. Free BSA-Cy7 conjugate was eliminated from the lung much more rapidly than the vaterite-encapsulated forms.

Tissue distribution of thus administered fluorescent marker followed a classical pathway comprising consecutive absorption, distribution, metabolism, and excretion. The fluorescence was first detected in the liver and then the kidneys [16].

The results presented in Ref. [16] demonstrate the high potential of submicron-sized vaterite to transport drugs via inhalation, thus providing a facile treatment of chronic and acute lung diseases since the studied particles are capable of delivering drugs deep in the respiratory portion of the lungs. Therefore, the vaterite encapsulation represents an excellent cause for COVID-19 therapeutics to substantially improve drug efficacy, release profile, and overall treatment outcome.

3.2.4. Transdermal delivery

Particulate formulations for transdermal drug delivery are one of the key focus areas in the research community. The transdermal delivery route allows drug self-administration and has other important advantages, such as pain-free and the digestive system bypass that are essential to avoid rapid degradation of active molecules and size-limited transport across the epithelium [89].

In vivo applications of porous $CaCO_3$ microparticles as carriers for biologically active compounds were recently extended to transdermal delivery. The rat model showed that the payload delivery route for topically applied submicron-sized porous vaterite particles comprised penetration and filling the hair follicles [17,58], where vaterite eventually recrystallized into non-porous polymorph and underwent bioresorption [17].

The penetration and filling effects could be enhanced with the therapeutic ultrasound treatment of the affected skin and followed by confocal laser scanning microscopy, visualizing the distribution of encapsulated fluorescent marker Cy7 in the time-resolved manner (Fig. 6). Fig. 6 illustrates the efficient transportation of the dye along the entire hair follicle down the bulb region. The payload release was observed over 11–12 days needed for recrystallization and complete dissolution of the $CaCO_3$ particles inside the hair follicles. After that, the fluorescent signal gradually decreased with time.

Analysis of the rats' urine samples proved systemic absorption of the fluorescent marker via hair follicles, wherein the Cy7 excretion kinetics in urine correlated strongly with intrafollicular storage kinetics and the particle degradation data. In a series of control experiments on Cy7 urinary excretion aimed to understand the effect of microencapsulation, the dye-loaded vaterite particles were applied topically without treating with ultrasound. In another setting, the dye was applied in its free form, followed by treatment with ultrasound. The results revealed that in both cases, the dye was essentially excreted within 24 h. Moreover, the intensity of fluorescence in the urine samples was at least five times lower than for the ultrasound-enhanced delivery of the Cy7-loaded vaterite, highlighting the importance of intrafollicular drug delivery compared to other transdermal transportation pathways [17].

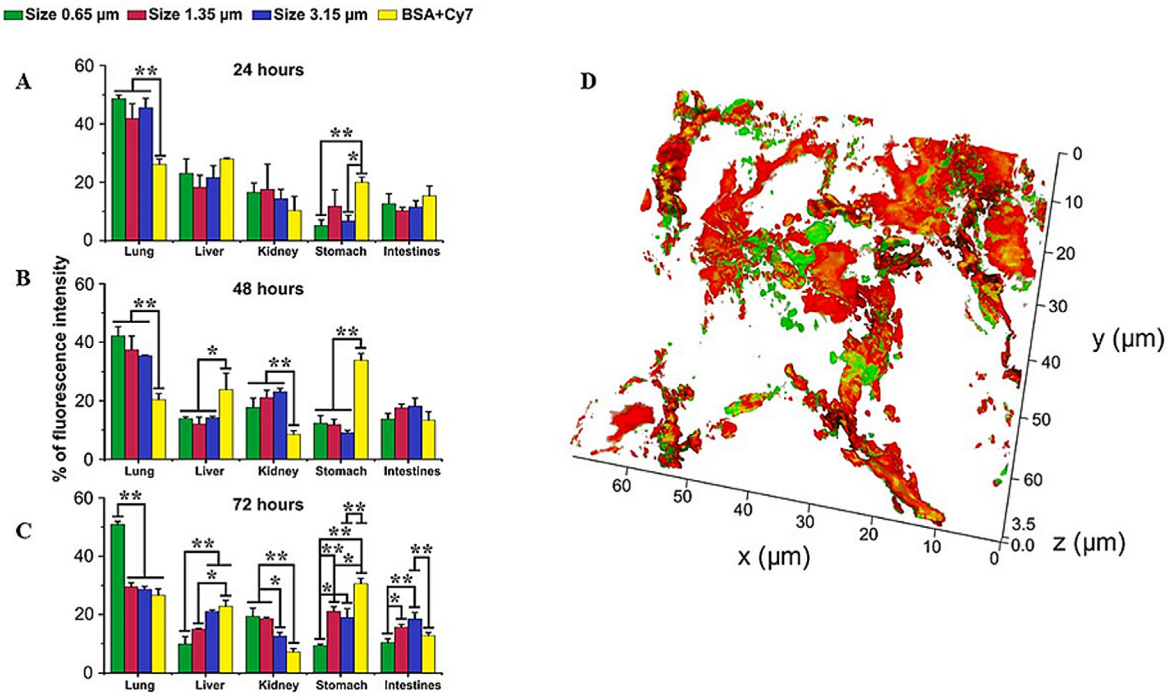

Fig. 5. Biodistribution of 0.65, 1.35, and 3.15 μm size vaterite particles loaded with BSA-Cy7 conjugate or BSA-Cy7 alone within various organs after 24 (A), 48 (B), and 72 h (C) intratracheal administration. Data are expressed as mean value ± SD, n = 3 mice per group. *p < 0.05, **p < 0.01. (D) 3D reconstruction of a lung cryosection fluorescent image. The BSA-Cy7-vaterite particles of the 0.65 μm were intratracheally administrated, and mice were sacrificed 20 min post-instillation. The red fluorescent signal represents the autofluorescence of capillaries; the green fluorescent signal corresponds to Cy7, areas where there is no fluorescent signal corresponding to the alveolar space. Adapted from Ref. [16]. *Copyright* © 2018, Frontiers Media SA.

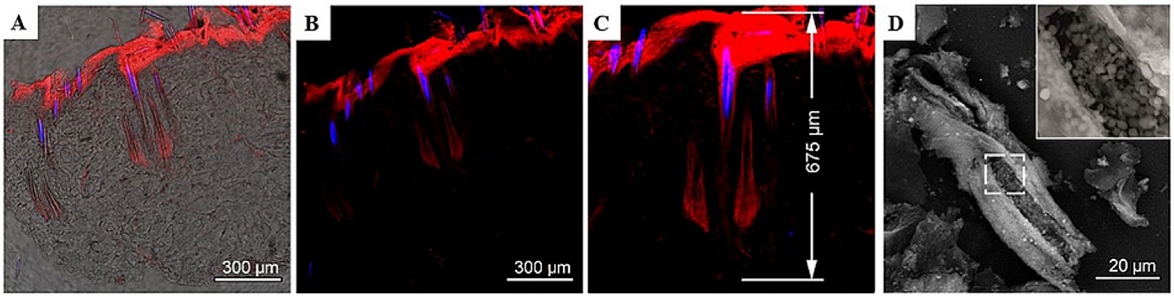

Fig. 6. Confocal laser scanning microscopy-images of frozen skin slices (a–c) and scanning electron microscope-image of the destructed root sheaths of a plucked hair (d) demonstrating *in vivo* intrafollicular penetration of Cy7-loaded calcium carbonate submicron particles. Blue fluorescent signal represents the autofluorescence of hair shafts, red fluorescence signal corresponds to the Cy7 marker demonstrating its distribution in tissue. Image (a) is an overlay of transmission and fluorescent images, (b) – fluorescent image, (c) – zoomed region of the image (b) enabling a clear determination of the penetration depth for Cy7-loaded calcium carbonate particles. Adapted with permission from Ref. [17]. *Copyright* © 2019, American Chemical Society.

In another study, Genina et al. [90] performed transdermal delivery of Fe_3O_4 nanoparticles loaded in micron-sized vaterite (4.0 ± 0.8 μm) in rats to demonstrate a possibility of creating the drug depots in the dermis. The particles were placed at a depth of about 300–400 μm through the channels formed by means of a minimally invasive procedure implying fractional microablation with the Er:YAG laser. The delivered vaterite particles were seen intact and maintaining spherical shape on histological sections prepared four days after administration. The histology study didn't detect any vaterite carrier seven days after the procedure, but the released Fe_3O_4 nanoparticles were seen residing at a depth of about 150 μm.

In the breakthrough research on vitiligo therapy, submicron porous $CaCO_3$ particles were used as an intrafollicular transport system for psoralen–ultraviolet tested on healthy human volunteers [91,92]. It was noticed that the encapsulated form provided drug accumulation inside the hair follicles resulting in a slower pigmentation buildup but a longer-term skin darkening effect and a more homogeneous pigmentation across the treated area compared to the free psoralen [92].

Topical application of submicron (~800 nm) $CaCO_3$ particles containing 4.9 wt% of naftifine was studied in mice. The particulate formulation deeply penetrated hair follicles and facilitated drug delivery deep into the dermis [60].

At this time, state-of-the-art research suggests that micron and submicron-sized vaterite particles constitute a transdermal drug delivery system of extremely high potential, aiming at both systemic and localized therapeutic effects.

4. Multi-drug-loaded vaterite: *in vitro* and *in vivo* delivery

As mentioned in Section 2.3, micro- and nanosized particles of vaterite are advantageous in the concomitant delivery of multiple drugs or active compounds with different structures and mechanisms of action. This Chapter provides further evidence of the bioeffects that are enhanced by co-delivered therapeutics' synergy *in vitro* and *in vivo*.

Wu et al. [37,52] and Gong et al. [53] obtained and extensively researched a $CaCO_3$-based delivery system for cancer combinatory therapy. The nanosized particles (<200 nm) were loaded with drug cocktails comprising different combinations of chemotherapeutics (doxorubicin and paclitaxel) and tariquidar, a compound undergoing extensive studies as an adjuvant against multidrug resistance in tumors. The bioeffect of tariquidar as an inhibitor of the membrane P-glycoprotein 1, also known as a multidrug resistance protein 1, signifies its use in co-delivery with the first-line chemotherapy drugs.

It has been shown that the dual drug-loaded nanoparticles carrying doxorubicin and tariquidar enhanced cell apoptosis of multidrug-resistant breast cancer MCF-7/ADR compared to that of individually loaded drugs [61,62]. The study involved four groups of cells treated with different encapsulated drug forms, a group treated with free doxorubicin, and a control group of untreated cells. The $CaCO_3$ nanoparticle-based compositions were as follows: carboxymethyl chitosan/$CaCO_3$/doxorubicin (CMC/$CaCO_3$/DOX), biotinylated carboxymethyl chitosan/$CaCO_3$/doxorubicin (BCMC/$CaCO_3$/DOX), carboxymethyl chitosan/$CaCO_3$/doxorubicin/tariquidar (CMC/$CaCO_3$/DOX/TQD), and biotinylated carboxymethyl chitosan/$CaCO_3$/doxorubicin/tariquidar (BCMC/$CaCO_3$/DOX/TQD). The treated and control cell groups were respectively analyzed by MTT assay to assess the viability and by Western blot to determine the content of apoptosis regulators, including the promoting factors, such as caspase 3, caspase 9, and glyceraldehyde 3-phosphate dehydrogenase (GAPDH), and inhibitors, such as Bcl-2 regulator protein and P-glycoprotein 1 (Fig. 7).

The BCMC/$CaCO_3$/DOX/TQR composition showed the highest inhibitory activity on the MCF-7/ADR cells due to the effective targeting provided by biotin moieties and the most efficient downregulation of the Bcl-2 regulator protein and P-glycoprotein 1 by co-delivered tariquidar. The synergistic effect of two therapeutics also resulted in the highest expression level of the apoptosis-promoting factors, caspase 3 and caspase 9 [61].

In another example, Zhao et al. [93] used $CaCO_3$ nanoparticles for co-delivery of the first-line chemotherapy drug, cisplatin, and anticarcinogen, selenium, to effectively treat osteosarcoma and

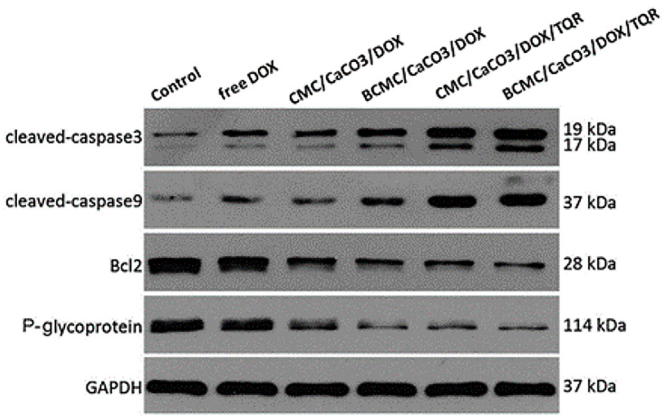

Fig. 7. Western blot analysis on MCF-7/ADR cells after treatment for 24 h. Reprinted with permission from Ref. [61]. *Copyright* © 2016, The Royal Society of Chemistry.

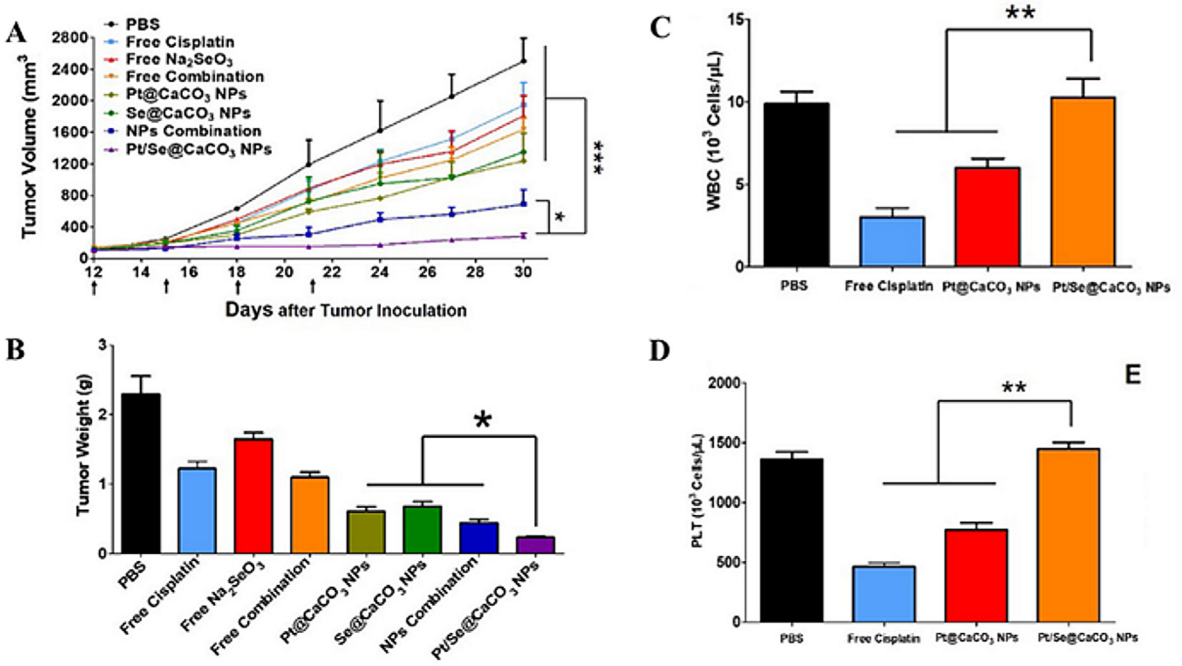

Fig. 8. (A) Growth curves of xenograft tumors treated with PBS, free cisplatin, free Na_2SeO_3, free combination, $Pt@CaCO_3$ NPs, $Se@CaCO_3$ NPs, NPs combination or $Pt/Se@CaCO_3$ NPs by tail vein injection (1 mg/kg Pt and 0.405 mg/kg Se). (B) Tumor weight of each group. (C) Level of WBC. (D) Level of PLT. Data are expressed as mean ± SEM (n = 6). *P < 0.05, **P < 0.01, ***P < 0.001. Adapted from Ref. [93]. *Copyright* © 2019, Elsevier B.V.

reduce side effects of cisplatin. A comparative biodistribution study of the co-encapsulated and free drug forms administered by tail vein injection in mice revealed the particles penetrated the tumor using the EPR effect, causing more than a ten-fold increase in the accumulation of platinum and selenium in the tumor after co-delivery by $CaCO_3$ compared with the free drugs.

The authors [93] further demonstrated that the co-delivered cisplatin and selenium had a synergistic effect at an optimized ratio of active components resulting in more potent tumor inhibition *in vitro* and *in vivo* (Fig. 8a and b). Furthermore, selenium protected normal tissues from chemotherapeutics toxicity. While the levels of white blood cells (WBC) and platelets (PLT) significantly declined in the groups of osteosarcoma xenograft mice treated with free cisplatin and the solo-loaded drug, the respective cell counts in the animals receiving co-encapsulates cisplatin and selenium were close to the untreated control (Fig. 8c and d) [93].

Cheng's group [94] has developed the precipitated $CaCO_3$ nanoparticles co-loaded with plasmid DNA and doxorubicin (LC = 1.0–1.1 wt %). $CaCO_3$ was synthesized in the presence of bioactive compounds and alginate that allowed the preparation of smaller particles with improved stability at physiological pH. Compared with the control particles without alginate, the alginate/$CaCO_3$/DNA/doxorubicin delivery system displayed a significantly improved gene transfection efficiency and the cancer cell inhibition effect *in vitro*.

The co-encapsulation approach can be an effective way to protect functional agents from enzymatic degradation and phagocytosis in the bloodstream. Zhao et al. [95] designed and assembled novel superparamagnetic microparticles based on vaterite crystals for magnetic-controlled targeted delivery and therapy. The multistage assembly process involved immobilization of doxorubicin, Au–DNA complex, and Fe_3O_4@silica nanoparticles into the porous mesocrystalline vaterite particles. Such microparticles possessed a distinct bioeffect *in vitro* confirmed by the successful transfection of HeLa and A549 cells with the green fluorescent protein plasmid reporter, wherein the delivered doxorubicin was visualized by

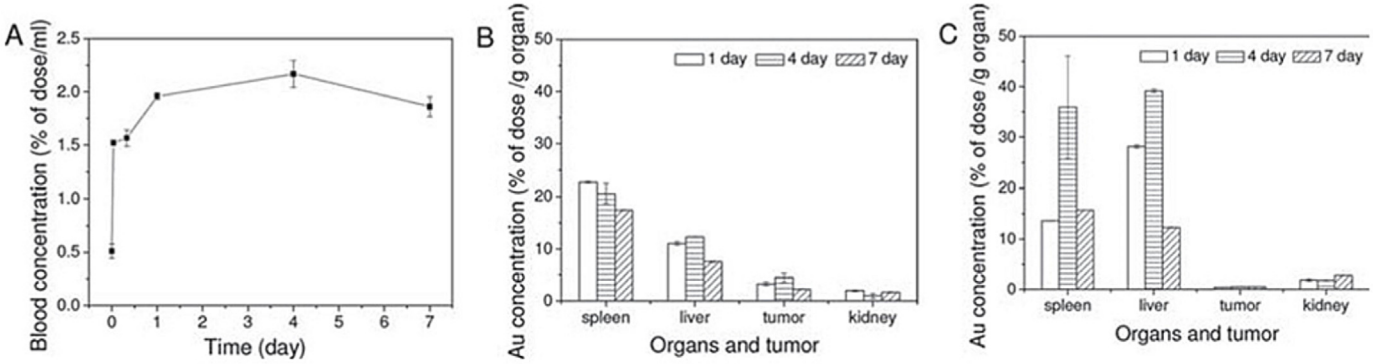

Fig. 9. Blood clearance (A) and biodistribution (B) of Au in the main organs and tumor after i.v. injection of the Au–$CaCO_3$ suspensions in the mouse tumor model over time. Biodistribution in main organs and tumor of Au after i.v. injection of Au nanoparticle suspensions in a mouse tumor model over time (C). Reprinted with permission from Ref. [95]. *Copyright* © 2010, WILEY-VCH Verlag GmbH & Co.

confocal microscopy.

After intravenous administration in mice, Au nanoparticles were released from vaterite and detected in blood in a constant concentration for at least four days (Fig. 9a). Moreover, the biodistribution study in the mouse tumor model, including various healthy organs and tumor tissue, demonstrated that Au nanoparticles, which were loaded in vaterite, accumulated in the tumor tissue tenfold more efficiently than free Au nanoparticles injected intravenously (Fig. 9b and c). The authors attributed the extended circulation of the Au nanoparticles in the bloodstream to the margination and attachment of nanoparticles and the vaterite-based microparticles to the blood vessel walls, which prevented them from clearance and extraction from the bloodstream [96]. As shown in Ref. [95], the biological distributions of doxorubicin and Au nanoparticles overlapped at the different time points, thus indicating a potential of the developed multidrug platform for the targeted delivery and/or co-delivery of multiple agents for biomedical imaging and therapy.

5. Conclusion

The nanoparticle-based technology of enhanced and/or targeted drug delivery has gained superior importance and popularity in a range of biomedical therapies, including treatment of COVID-19 via vaccines delivered by lipid nanoparticles. The current manuscript provided the scope of potential utility for calcium carbonate in its vaterite polymorph – a biocompatible, safe, multifaceted, and robust delivery platform in its inception stage of clinical applications. Additional benefits of $CaCO_3$-based delivery systems include bioavailability, low cost, and physiologically driven biodegradability leading to an extended cargo release at the site of action. Due to significant porosity, surface area, and rapid decomposition under relatively mild conditions, vaterite is considered a prospective candidate for formulations with controlled drug release of high efficacy. The vaterite micron and submicron particles have been successfully applied in various methods of drug administration, e.g., oral, injections, and through other parenteral routes. The functionalization of the vaterite porous particles with diagnostic and therapeutic agents, summarized in this review, demonstrates a wide range of its utility as an efficient site-specific drug carrier with minor or even absent toxicity for healthy cells and tissues.

There is no universally effective loading method, and encapsulation in vaterite typically involves the design and further optimization of the loading protocol depending on the properties of the particular bioactive. This manuscript discussed the main parameters influencing the vaterite loading and highlighted technical solutions toward increased efficacy, holding promise for future industrial utilization (e.g., freezing-induced loading, combined adsorption/centrifugation, and enhancing the vaterite particles with adjuvant components that can beneficially interact with the loaded bioactives).

It should be noted that vaterite micron and submicron-sized particles are extensively used as a sacrificial pre-loading template for biodegradable polymeric multilayer capsules. Thus, the aspects of vaterite loading optimization and enhancement discussed in this review are fully applicable for further advances in the development of those targeted drug delivery systems.

An additional and far more important feature of the current use of $CaCO_3$ in its vaterite form for drug delivery is the commercialization and marketing of such particles produced in significant quantities. This capability is already reaching its breakthrough: several commercial entities are producing vaterite in multi-kilogram amounts, with proprietary technologies granting the stability and the desired mode of action.

Data statement

Due to the manuscript being a review paper, raw data would not be shared.

Declaration of competing interest

The authors declare that they have no known competing financial interests or personal relationships that could have appeared to influence the work reported in this paper.

Acknowledgment

The work was supported by the Russian Science Foundation (Project # 21-74-10058, Sechenov First Moscow State Medical University) in the part of the overview of the most recent advances in vaterite application for *in vivo* delivery of therapeutics via injection administration and by the Ministry of Science and Higher Education of the Russian Federation within the State assignment FSRC “Crystallography and Photonics” RAS in part of systematization of factors affecting the loading capacity of $CaCO_3$ particles.

References

[1] H. He, Y. Lu, J. Qi, Q. Zhu, Z. Chen, W. Wu, Adapting liposomes for oral drug delivery, Acta Pharm. Sin. B. 9 (2019) 36–48, https://doi.org/10.1016/j.apsb.2018.06.005.

[2] D.E. Cohn, W.S. Shimp, The cost implications of the use of pegylated liposomal doxorubicin when choosing an anthracycline for the treatment of platinum-resistant ovarian cancer: a low-value intervention? Gynecol. Oncol. Rep. 13 (2015) 47–48, https://doi.org/10.1016/j.gore.2015.06.009.

[3] Y. Ngan, M. Gupta, A comparison between liposomal and nonliposomal formulations of doxorubicin in the treatment of cancer: an updated review, Arch. Pharm. Pract. 7 (2016) 1, https://doi.org/10.4103/2045-080x.174930.

[4] H.H.L. Borba, L.M. Steimbach, B.S. Riveros, F.S. Tonin, V.L. Ferreira, B.A. de Q. Bagatim, G. Balan, R. Pontarolo, A. Wiens, Cost-effectiveness of amphotericin B formulations in the treatment of systemic fungal infections, Mycoses 61 (2018) 754–763, https://doi.org/10.1111/myc.12801.

[5] A. Vikulina, D.V. Voronin, R.F. Fakhrullin, V.A. Vinokurov, D. Volodkin, Naturally derived nano- and micro- drug delivery vehicles: halloysite, vaterite and nanocellulose, New J. Chem. (2020), https://doi.org/10.1039/C9NJ06470B.

[6] A. Trofimov, A. Ivanova, M. Zyuzin, A. Timin, Porous Inorganic Carriers Based on Silica, Calcium Carbonate and Calcium Phosphate for Controlled/Modulated Drug Delivery: Fresh Outlook and Future Perspectives, 2018, https://doi.org/10.3390/pharmaceutics10040167.

[7] M. Devenney, M. Fernandez, S.O. Morgan, Non-cementitious Compositions Comprising Vaterite and Methods Thereof, 2013.

[8] V.K.K. Paravastu, S.R. Yarraguntla, A. Suvvari, Role of nanocomposites in drug delivery, GSC Biol. Pharm. Sci. 8 (2019), https://doi.org/10.30574/gscbps.2019.8.3.0150, 094–103.

[9] G. Cavallaro, G. Lazzara, R. Fakhrullin, Mesoporous inorganic nanoscale particles for drug adsorption and controlled release, Ther. Deliv. 9 (2018) 287–301, https://doi.org/10.4155/tde-2017-0120.

[10] S. Maleki Dizaj, S. Sharifi, E. Ahmadian, A. Eftekhari, K. Adibkia, F. Lotfipour, An update on calcium carbonate nanoparticles as cancer drug/gene delivery system, Expet Opin. Drug Deliv. 16 (2019) 331–345, https://doi.org/10.1080/17425247.2019.1587408.

[11] Y. Zhao, Z. Luo, M. Li, Q. Qu, X. Ma, S.H. Yu, Y. Zhao, A preloaded amorphous calcium carbonate/doxorubicin@silica nanoreactor for pH-responsive delivery of an anticancer drug, Angew. Chem. Int. Ed. 54 (2015) 919–922, https://doi.org/10.1002/anie.201408510.

[12] N.G. Balabushevich, E.A. Kovalenko, E.V. Mikhalchik, L.Y. Filatova, D. Volodkin, A.S. Vikulina, Mucin adsorption on vaterite CaCO3 microcrystals for the prediction of mucoadhesive properties, J. Colloid Interface Sci. 545 (2019) 330–339, https://doi.org/10.1016/j.jcis.2019.03.042.

[13] N.G. Balabushevich, E.A. Sholina, E.V. Mikhalchik, L.Y. Filatova, A.S. Vikulina, D. Volodkin, Self-assembled mucin-containing microcarriers via hard templating on CaCO3crystals, Micromachines 9 (2018) 1–16, https://doi.org/10.3390/mi9060307.

[14] I. Marchenko, T. Borodina, D. Trushina, I. Rassokhina, Y. Volkova, V. Shirinian, I. Zavarzin, A. Gogin, T. Bukreeva, Mesoporous particle-based microcontainers for intranasal delivery of imidazopyridine drugs, J. Microencapsul. 35 (2018) 657–666, https://doi.org/10.1080/02652048.2019.1571642.

[15] P.V. Binevski, N.G. Balabushevich, V.I. Uvarova, A.S. Vikulina, D. Volodkin, Biofriendly encapsulation of superoxide dismutase into vaterite CaCO3 crystals. Enzyme activity, release mechanism, and perspectives for ophthalmology,

Colloids Surf. B Biointerfaces 181 (2019) 437–449, https://doi.org/10.1016/j.colsurfb.2019.05.077.
[16] O. Gusliakova, E.N. Atochina-Vasserman, O. Sindeeva, S. Sindeev, S. Pinyaev, N. Pyataev, V. Revin, G.B. Sukhorukov, D. Gorin, A.J. Gow, Use of submicron vaterite particles serves as an effective delivery vehicle to the respiratory portion of the lung, Front. Pharmacol. 9 (2018) 1–13, https://doi.org/10.3389/fphar.2018.00559.
[17] Y.I. Svenskaya, E.A. Genina, B.V. Parakhonskiy, E. Lengert, E.E. Talnikova, G.S. Terentyuk, S.R. Utz, D.A. Gorin, V.V. Tuchin, G. Sukhorukov, A simple non-invasive approach towards efficient transdermal drug delivery based on biodegradable particulate system, ACS Appl. Mater. Interfaces (2019), https://doi.org/10.1021/acsami.9b04305 acsami.9b04305.
[18] D. Liu, G. Jiang, W. Yu, L. Li, Z. Tong, X. Kong, J. Yao, Oral delivery of insulin using CaCO3-based composite nanocarriers with hyaluronic acid coatings, Mater. Lett. 188 (2017) 263–266, https://doi.org/10.1016/j.matlet.2016.10.117.
[19] D. Volodkin, CaCO3 templated micro-beads and -capsules for bioapplications, Adv. Colloid Interface Sci. 207 (2014) 306–324, https://doi.org/10.1016/j.cis.2014.04.001.
[20] S.V. German, M.V. Novoselova, D.N. Bratashov, P.A. Demina, V.S. Atkin, D.V. Voronin, B.N. Khlebtsov, B.V. Parakhonskiy, G.B. Sukhorukov, D.A. Gorin, High-efficiency freezing-induced loading of inorganic nanoparticles and proteins into micron- and submicron-sized porous particles, Sci. Rep. 8 (2018) 17763, https://doi.org/10.1038/s41598-018-35846-x.
[21] P.A. Demina, D.V. Voronin, E.V. Lengert, A.M. Abramova, V.S. Atkin, B.V. Nabatov, A.P. Semenov, D.G. Shchukin, T.V. Bukreeva, Freezing-Induced Loading of TiO2 into Porous Vaterite Microparticles: Preparation of CaCO3/TiO2 Composites as Templates to Assemble UV-Responsive Microcapsules for Wastewater Treatment, ACS Omega, 2020, https://doi.org/10.1021/acsomega.9b03819.
[22] A.I. Petrov, D. V Volodkin, G.B. Sukhorukov, Protein-calcium carbonate coprecipitation: a tool for protein encapsulation, Biotechnol. Prog. 21 (2008) 918–925, https://doi.org/10.1021/bp0495825.
[23] A.S. Vikulina, N.A. Feoktistova, N.G. Balabushevich, A.G. Skirtach, D. Volodkin, The mechanism of catalase loading into porous vaterite CaCO3 crystals by co-synthesis, Phys. Chem. Chem. Phys. 20 (2018) 8822–8831, https://doi.org/10.1039/c7cp07836f.
[24] D.B. Trushina, T.V. Bukreeva, M.V. Kovalchuk, M.N. Antipina, CaCO3 vaterite microparticles for biomedical and personal care applications, Mater. Sci. Eng. C 45 (2014) 644–658, https://doi.org/10.1016/j.msec.2014.04.050.
[25] N.M. Elbaz, A. Owen, S. Rannard, T.O. McDonald, Controlled synthesis of calcium carbonate nanoparticles and stimuli-responsive multi-layered nanocapsules for oral drug delivery, Int. J. Pharm. 574 (2020) 118866, https://doi.org/10.1016/j.ijpharm.2019.118866.
[26] N. Qiu, H. Yin, B. Ji, N. Klauke, A. Glidle, Y. Zhang, H. Song, L. Cai, L. Ma, G. Wang, L. Chen, W. Wang, Calcium carbonate microspheres as carriers for the anticancer drug camptothecin, Mater. Sci. Eng. C 32 (2012) 2634–2640, https://doi.org/10.1016/j.msec.2012.08.026.
[27] S.P. Dunuweera, R.M.G. Rajapakse, Encapsulation of anticancer drug cisplatin in vaterite polymorph of calcium carbonate nanoparticles for targeted delivery and slow release, Biomed. Phys. Eng. Expr. 4 (2017), 015017, https://doi.org/10.1088/2057-1976/aa9719.
[28] J.L. Wu, C.Q. Wang, R.X. Zhuo, S.X. Cheng, Multi-drug delivery system based on alginate/calcium carbonate hybrid nanoparticles for combination chemotherapy, Colloids Surf. B Biointerfaces 123 (2014) 498–505, https://doi.org/10.1016/j.colsurfb.2014.09.047.
[29] C. Wang, C. He, Z. Tong, X. Liu, B. Ren, F. Zeng, Combination of adsorption by porous CaCO3 microparticles and encapsulation by polyelectrolyte multilayer films for sustained drug delivery, Int. J. Pharm. 308 (2006) 160–167, https://doi.org/10.1016/j.ijpharm.2005.11.004.
[30] C. Charnay, S. Bégu, C. Tourné-Péteilh, L. Nicole, D.A. Lerner, J.M. Devoisselle, Inclusion of ibuprofen in mesoporous templated silica: drug loading and release property, Eur. J. Pharm. Biopharm. 57 (2004) 533–540, https://doi.org/10.1016/j.ejpb.2003.12.007.
[31] N.A. Feoktistova, A.S. Vikulina, N.G. Balabushevich, A.G. Skirtach, D. Volodkin, Bioactivity of catalase loaded into vaterite CaCO3 crystals via adsorption and co-synthesis, Mater. Des. 185 (2020) 108223, https://doi.org/10.1016/j.matdes.2019.108223.
[32] Z. She, C. Wang, J. Li, G.B. Sukhorukov, M.N. Antipina, Encapsulation of basic fibroblast growth factor by polyelectrolyte multilayer microcapsules and its controlled release for enhancing cell proliferation, Biomacromolecules 13 (2012) 2174–2180, https://doi.org/10.1021/bm3005879.
[33] M. Kakran, M. Muratani, W.J. Tng, H. Liang, D.B. Trushina, G.B. Sukhorukov, H.H. Ng, M.N. Antipina, Layered polymeric capsules inhibiting the activity of RNases for intracellular delivery of messenger RNA, J. Mater. Chem. B. 3 (2015) 5842–5848, https://doi.org/10.1039/C5TB00615E.
[34] Y. Svenskaya, B. Parakhonskiy, A. Haase, V. Atkin, E. Lukyanets, D. Gorin, R. Antolini, Anticancer drug delivery system based on calcium carbonate particles loaded with a photosensitizer, Biophys. Chem. 182 (2013) 11–15, https://doi.org/10.1016/j.bpc.2013.07.006.
[35] Y.I. Svenskaya, N.A. Navolokin, A.B. Bucharskaya, G.S. Terentyuk, A.O. Kuz'mina, M.M. Burashnikova, G.N. Maslyakova, E.A. Lukyanets, D.A. Gorin, Calcium carbonate microparticles containing a photosensitizer photosens: preparation, ultrasound stimulated dye release, and *in vivo* application, Nanotechnol. Russ. 9 (2014) 398–409, https://doi.org/10.1134/S1995078014040181.
[36] T.N. Borodina, L.D. Rumsh, S.M. Kunizhev, G.B. Sukhorukov, G.N. Vorozhtsov, B.M. Feldman, A.V. Rusanova, T.V. Vasil'eva, S.M. Strukova, E.A. Markvicheva, Entrapment of herbal extracts into biodegradable microcapsules, Biochem. Suppl. Ser. B Biomed. Chem. 2 (2008) 176–182, https://doi.org/10.1134/s199075080802008x.
[37] A. Abalymov, L. Van Poelvoorde, V.S. Atkin, A.G. Skirtach, M. Konrad, B. Parakhonskiy, Alkaline phosphatase delivery system based on calcium carbonate carriers for acceleration of ossification, ACS Appl. Bio Mater. (2020), https://doi.org/10.1021/acsabm.0c00053 acsabm.0c00053.
[38] D.B. Trushina, T.V. Bukreeva, M.N. Antipina, Size-controlled synthesis of vaterite calcium carbonate by the mixing method: aiming for nanosized particles, Cryst. Growth Des. 16 (2016) 1311–1319, https://doi.org/10.1021/acs.cgd.5b01422.
[39] Y.I. Svenskaya, H. Fattah, O.A. Inozemtseva, A.G. Ivanova, S.N. Shtykov, D.A. Gorin, B.V. Parakhonskiy, Key parameters for size- and shape-controlled synthesis of vaterite particles, Cryst. Growth Des. 18 (2018) 331–337, https://doi.org/10.1021/acs.cgd.7b01328.
[40] S. Donatan, A. Yashchenok, N. Khan, B. Parakhonskiy, M. Cocquyt, B. El Pinchasik, D. Khalenkow, H. Möhwald, M. Konrad, A. Skirtach, Loading capacity versus enzyme activity in anisotropic and spherical calcium carbonate microparticles, ACS Appl. Mater. Interfaces 8 (2016) 14284–14292, https://doi.org/10.1021/acsami.6b03492.
[41] B.V. Parakhonskiy, A.M. Yashchenok, S. Donatan, D. V Volodkin, F. Tessarolo, R. Antolini, H. Möhwald, A.G. Skirtach, Macromolecule loading into spherical, elliptical, star-like and cubic calcium carbonate carriers, ChemPhysChem 15 (2014) 2817–2822, https://doi.org/10.1002/cphc.201402136.
[42] A. Vikulina, J. Webster, D. Voronin, E. Ivanov, R. Fakhrullin, V. Vinokurov, D. Volodkin, Mesoporous additive-free vaterite CaCO3 crystals of untypical sizes: from submicron to Giant, Mater. Des. 197 (2021) 109220, https://doi.org/10.1016/j.matdes.2020.109220.
[43] Q. Dong, J. Li, L. Cui, H. Jian, A. Wang, S. Bai, Using porous CaCO3/hyaluronic acid nanocages to accommodate hydrophobic photosensitizer in aqueous media for photodynamic therapy, Colloid. Surf. A Physicochem. Eng. Asp. 516 (2017) 190–198, https://doi.org/10.1016/j.colsurfa.2016.12.027.
[44] D.B. Trushina, T.N. Borodina, V. V Artemov, T. V Bukreeva, Immobilization of photoditazine on vaterite porous particles and analysis of the system stability in model media, Tech. Phys. 63 (2018) 1387–1393, https://doi.org/10.1134/S1063784218090220.
[45] N.G. Balabushevich, A.V. Lopez de Guerenu, N.A. Feoktistova, D. Volodkin, Protein loading into porous CaCO 3 microspheres: adsorption equilibrium and bioactivity retention, Phys. Chem. Chem. Phys. 17 (2015) 2523–2530, https://doi.org/10.1039/C4CP04567J.
[46] L.N. Hassani, F. Hindré, T. Beuvier, B. Calvignac, N. Lautram, A. Gibaud, F. Boury, Lysozyme encapsulation into nanostructured CaCO3 microparticles using a supercritical CO2 process and comparison with the normal route, J. Mater. Chem. B. 1 (2013) 4011, https://doi.org/10.1039/c3tb20467g.
[47] N. Osada, C. Otsuka, Y. Nishikawa, T. Kasuga, Protein adsorption behaviors on siloxane-containing vaterite particles, Mater. Lett. 264 (2020) 127280, https://doi.org/10.1016/j.matlet.2019.127280.
[48] P. Shi, S. Luo, B. Voit, D. Appelhans, X. Zan, A facile and efficient strategy to encapsulate the model basic protein lysozyme into porous CaCO3, J. Mater. Chem. B. 6 (2018) 4205–4215, https://doi.org/10.1039/c8tb00312b.
[49] G. Choukrani, B. Maharjan, C.H. Park, C.S. Kim, A.R. Kurup Sasikala, Biocompatible superparamagnetic sub-micron vaterite particles for thermo-chemotherapy: from controlled design to *in vitro* anticancer synergism, Mater. Sci. Eng. C 106 (2020) 110226, https://doi.org/10.1016/j.msec.2019.110226.
[50] N.A. Feoktistova, N.G. Balabushevich, A.G. Skirtach, D. Volodkin, A.S. Vikulina, Inter-protein interactions govern protein loading into porous vaterite CaCO 3 crystals, Phys. Chem. Chem. Phys. 22 (2020) 9713–9722, https://doi.org/10.1039/D0CP00404A.
[51] P. Rivera-Gil, S. De Koker, B.G. De Geest, W.J. Parak, Intracellular processing of proteins mediated by biodegradable polyelectrolyte capsules, Nano Lett. 9 (2009) 4398–4402, https://doi.org/10.1021/nl902697j.
[52] E. Kilic, M.V. Novoselova, S.H. Lim, N.A. Pyataev, S.I. Pinyaev, O.A. Kulikov, O.A. Sindeeva, O.A. Mayorova, R. Murney, M.N. Antipina, B. Haigh, G.B. Sukhorukov, M.V. Kiryukhin, Formulation for oral delivery of lactoferrin based on bovine serum albumin and tannic acid multilayer microcapsules, Sci. Rep. 7 (2017) 44159, https://doi.org/10.1038/srep44159.
[53] V.A. Aniol, I. Novitskaia, T.N. Borodina, T.V. Bukreeva, N.A. Lazareva, I.V. Moiseeva, M.V. Onufriev, M.I. Stepanichev, A.A. Iakovlev, A.B. Gekht, O.K. Granstrem, N.V. Guliaeva, [Evaluation of antiepileptic effects of cortexin in a model of convulsions], Zh. Nevrol. Psikhiatr. Im. S S Korsakova 111 (2011).
[54] Y. Ueno, H. Futagawa, Y. Takagi, A. Ueno, Y. Mizushima, Drug-incorporating calcium carbonate nanoparticles for a new delivery system, J. Contr. Release 103 (2005) 93–98, https://doi.org/10.1016/j.jconrel.2004.11.015.
[55] J. Song, R. Wang, Z. Liu, H. Zhang, Preparation and characterization of calcium carbonate microspheres and their potential application as drug carriers, Mol. Med. Rep. 17 (2018) 8403–8408, https://doi.org/10.3892/mmr.2018.8879.
[56] H. Peng, K. Li, T. Wang, J. Wang, J. Wang, R. Zhu, D. Sun, S. Wang, Preparation of hierarchical mesoporous CaCO3 by a facile binary solvent approach as anticancer drug carrier for etoposide, Nanoscale Res. Lett. 8 (2013) 321,

https://doi.org/10.1186/1556-276X-8-321.
[57] Y.I. Svenskaya, A.M. Pavlov, D.A. Gorin, D.J. Gould, B.V. Parakhonskiy, G.B. Sukhorukov, Photodynamic therapy platform based on localized delivery of photosensitizer by vaterite submicron particles, Colloids Surf. B Biointerfaces 146 (2016) 171–179, https://doi.org/10.1016/j.colsurfb.2016.05.090.
[58] E. Lengert, R. Verkhovskii, N. Yurasov, E. Genina, Y. Svenskaya, Mesoporous carriers for transdermal delivery of antifungal drug, Mater. Lett. 248 (2019) 211–213, https://doi.org/10.1016/j.matlet.2019.04.028.
[59] O.I. Gusliakova, E.V. Lengert, V.S. Atkin, V.V. Tuchin, Y.I. Svenskaya, Spectral monitoring of naftifine immobilization into submicron vaterite particles, Opt Spectrosc. 126 (2019) 539–544, https://doi.org/10.1134/S0030400X19050114.
[60] O. Gusliakova, R. Verkhovskii, A. Abalymov, E. Lengert, A. Kozlova, V. Atkin, O. Nechaeva, A. Morrison, V. Tuchin, Y. Svenskaya, Transdermal platform for the delivery of the antifungal drug naftifine hydrochloride based on porous vaterite particles, Mater. Sci. Eng. C 119 (2021) 111428, https://doi.org/10.1016/j.msec.2020.111428.
[61] J.-L. Wu, X.-Y. He, P.-Y. Jiang, M.-Q. Gong, R.-X. Zhuo, S.-X. Cheng, Biotinylated carboxymethyl chitosan/CaCO3 hybrid nanoparticles for targeted drug delivery to overcome tumor drug resistance, RSC Adv. 6 (2016) 69083–69093, https://doi.org/10.1039/C6RA04219H.
[62] M.Q. Gong, J.L. Wu, B. Chen, R.X. Zhuo, S.X. Cheng, Self-assembled polymer/inorganic hybrid nanovesicles for multiple drug delivery to overcome drug resistance in cancer chemotherapy, Langmuir 31 (2015) 5115–5122, https://doi.org/10.1021/acs.langmuir.5b00542.
[63] N. Sudareva, O. Suvorova, N. Saprykina, N. Smirnova, P. Bel'tyukov, S. Petunov, A. Radilov, A. Vilesov, Two-level delivery systems based on CaCO 3 cores for oral administration of therapeutic peptides, J. Microencapsul. 35 (2018) 619–634, https://doi.org/10.1080/02652048.2018.1559247.
[64] C. Peng, Q. Zhao, C. Gao, Sustained delivery of doxorubicin by porous CaCO3 and chitosan/alginate multilayers-coated CaCO3 microparticles, Colloid. Surf. A Physicochem. Eng. Asp. 353 (2010) 132–139, https://doi.org/10.1016/j.colsurfa.2009.11.004.
[65] A. Wang, Y. Yang, X. Zhang, X. Liu, W. Cui, J. Li, Gelatin-assisted synthesis of vaterite nanoparticles with higher surface area and porosity as anticancer drug containers *in vitro*, Chempluschem 81 (2016) 194–201, https://doi.org/10.1002/cplu.201500515.
[66] X. Ying, C. Shan, K. Jiang, Z. Chen, Y. Du, Intracellular pH-sensitive delivery CaCO 3 nanoparticles templated by hydrophobic modified starch micelles, RSC Adv. 4 (2014) 10841–10844, https://doi.org/10.1039/C3RA47501H.
[67] L. Li, Y. Yang, Y. Lv, P. Yin, T. Lei, Porous calcite CaCO3 microspheres: preparation, characterization and release behavior as doxorubicin carrier, Colloids Surf. B Biointerfaces 186 (2020) 1–7, https://doi.org/10.1016/j.colsurfb.2019.110720.
[68] V.E. Bosio, M.L. Cacicedo, B. Calvignac, I. León, T. Beuvier, F. Boury, G.R. Castro, Synthesis and characterization of CaCO3-biopolymer hybrid nanoporous microparticles for controlled release of doxorubicin, Colloids Surf. B Biointerfaces 123 (2014) 158–169, https://doi.org/10.1016/j.colsurfb.2014.09.011.
[69] A. Zou, Y. Chen, M. Huo, J. Wang, Y. Zhang, J. Zhou, Q. Zhang, In vivo studies of octreotide-modified N-octyl-O, N-carboxymethyl chitosan micelles loaded with doxorubicin for tumor-targeted delivery, J. Pharmacol. Sci. 102 (2013) 126–135, https://doi.org/10.1002/jps.23341.
[70] N.G. Balabushevich, E.A. Kovalenko, I.M. Le-Deygen, L.Y. Filatova, D. Volodkin, A.S. Vikulina, Hybrid CaCO3-mucin crystals: effective approach for loading and controlled release of cationic drugs, Mater. Des. 182 (2019) 108020, https://doi.org/10.1016/j.matdes.2019.108020.
[71] J. Xue, X. Li, Q. Li, J. Lyu, W. Wang, L. Zhuang, Y. Xu, Magnetic drug-loaded osteoinductive Fe3O4/CaCO3 hybrid microspheres system: efficient for sustained release of antibiotics, J. Phys. D Appl. Phys. (2020), https://doi.org/10.1088/1361-6463/ab7bb2, 0–14.
[72] P. Singh, K. Sen, Drug delivery of sulphanilamide using modified porous calcium carbonate, Colloid Polym. Sci. 296 (2018) 1711–1718, https://doi.org/10.1007/s00396-018-4392-x.
[73] V. Vergaro, P. Papadia, S. Leporatti, S.A. De Pascali, F.P. Fanizzi, G. Ciccarella, Synthesis of biocompatible polymeric nano-capsules based on calcium carbonate: a potential cisplatin delivery system, J. Inorg. Biochem. 153 (2015) 284–292, https://doi.org/10.1016/j.jinorgbio.2015.10.014.
[74] S. V German, G.S. Budylin, E.A. Shirshin, D.A. Gorin, Advanced technique for *in situ* Raman spectroscopy monitoring of the freezing-induced loading process, Langmuir 37 (2021) 1365–1371, https://doi.org/10.1021/acs.langmuir.0c02593.
[75] B.V. Parakhonskiy, A. Abalymov, A. Ivanova, D. Khalenkow, A. Skirtach, Magnetic and silver nanoparticle functionalized calcium carbonate particles—dual functionality of versatile, movable delivery carriers which can surface-enhance Raman signals, J. Appl. Phys. 126 (2019), https://doi.org/10.1063/1.5111973.
[76] M.V. Novoselova, D.V. Voronin, T.O. Abakumova, P.A. Demina, A.V. Petrov, V.V. Petrov, T.S. Zatsepin, G.B. Sukhorukov, D.A. Gorin, Focused ultrasound-mediated fluorescence of composite microcapsules loaded with magnetite nanoparticles: *In vitro* and *in vivo* study, Colloids Surf. B Biointerfaces 181 (2019) 680–687, https://doi.org/10.1016/j.colsurfb.2019.06.025.
[77] P.A. Demina, A.A. Abalymov, D.V. Voronin, A.V. Sadovnikov, M.V. Lomova, Highly-magnetic mineral protein-tannin vehicles with anti-breast cancer activity, Mater. Chem. Front. 5 (2021), https://doi.org/10.1039/d0qm00732c, 2007–2018.
[78] A. Som, R. Raliya, L. Tian, W. Akers, J.E. Ippolito, S. Singamaneni, P. Biswas, S. Achilefu, Monodispersed calcium carbonate nanoparticles modulate local pH and inhibit tumor growth *in vivo*, Nanoscale 8 (2016) 12639–12647, https://doi.org/10.1039/C5NR06162H.
[79] A. Som, R. Raliya, K. Paranandi, R.A. High, N. Reed, S.C. Beeman, M. Brandenburg, G. Sudlow, J.L. Prior, W. Akers, A.Y. Mah-Som, L. Habimana-Griffin, J. Garbow, J.E. Ippolito, M.D. Pagel, P. Biswas, S. Achilefu, Calcium carbonate nanoparticles stimulate tumor metabolic reprogramming and modulate tumor metastasis, Nanomedicine 14 (2019) 169–182, https://doi.org/10.2217/nnm-2018-0302.
[80] S.K. Kim, M.B. Foote, L. Huang, Targeted delivery of EV peptide to tumor cell cytoplasm using lipid coated calcium carbonate nanoparticles, Cancer Lett. 334 (2013) 311–318, https://doi.org/10.1016/j.canlet.2012.07.011.
[81] Y. Zhang, L. Cai, D. Li, Y. Lao, D. Liu, M. Li, J. Ding, X. Chen, Tumor microenvironment-responsive hyaluronate-calcium carbonate hybrid nanoparticle enables effective chemotherapy for primary and advanced osteosarcomas, Nano Res. 11 (2018) 4806–4822, https://doi.org/10.1007/s12274-018-2066-0.
[82] N. Sun, D. Wang, G. Yao, X. Li, T. Mei, X. Zhou, K.-Y. Wong, B. Jiang, Z. Fang, pH-dependent and cathepsin B activable CaCO3 nanoprobe for targeted *in vivo* tumor imaging, Int. J. Nanomed. 14 (2019) 4309–4317, https://doi.org/10.2147/IJN.S201722.
[83] N.N. Sudareva, P. V Popryadukhin, N.N. Saprykina, O.M. Suvorova, G.Y. Yukina, O.V. Galibin, A.D. Vilesov, CaCO3 vaterites as components of target drug delivery systems, Cell Ther. Transplant 9 (2020) 13–19, https://doi.org/10.18620/ctt-1866-8836-2020-9-2-13-19.
[84] P.V. Popryadukhin, N.N. Sudareva, O.M. Suvorova, G.Y. Yukina, E.G. Sukhorukova, N.N. Saprykina, Morphology of porous CACO3 vaterites as components of target drug delivery systems in rat muscle tissue, Cell Tissue Biol. 15 (2021) 208–213, https://doi.org/10.1134/S1990519X21020061.
[85] S. Haruta, T. Hanafusa, H. Fukase, H. Miyajima, T. Oki, An effective absorption behavior of insulin for diabetic treatment following intranasal delivery using porous spherical calcium carbonate in monkeys and healthy human volunteers, Diabetes Technol. Therapeut. 5 (2003) 1–9, https://doi.org/10.1089/152091503763816409.
[86] F. Ishikawa, M. Murano, M. Hiraishi, T. Yamaguchi, I. Tamai, A. Tsuji, Insoluble powder formulation as an effective nasal drug delivery system, Pharm. Res. (N. Y.) 19 (2002) 1097–1104, https://doi.org/10.1023/A:1019881706159.
[87] T.V. Bukreeva, I.V. Marchenko, T.N. Borodina, I.V. Degtev, S.L. Sitnikov, Y.V. Moiseeva, N.V. Gulyaeva, M.V. Kovalchuk, Calcium carbonate and titanium dioxide particles as a basis for container fabrication for brain delivery of compounds, Dokl. Phys. Chem. 440 (2011) 165–167, https://doi.org/10.1134/S001250161109003X.
[88] T. Borodina, I. Marchenko, D. Trushina, Y. Volkova, V. Shirinian, I. Zavarzin, E. Kondrakhin, G. Kovalev, M. Kovalchuk, T. Bukreeva, A novel formulation of zolpidem for direct nose-to-brain delivery: synthesis, encapsulation and intranasal administration to mice, J. Pharm. Pharmacol. 70 (2018) 1164–1173, https://doi.org/10.1111/jphp.12958.
[89] A. Alkilani, M.T. McCrudden, R. Donnelly, Transdermal drug delivery: innovative pharmaceutical developments based on disruption of the barrier properties of the stratum corneum, Pharmaceutics 7 (2015) 438–470, https://doi.org/10.3390/pharmaceutics7040438.
[90] E.A. Genina, Y.I. Svenskaya, I.Y. Yanina, L.E. Dolotov, N.A. Navolokin, A.N. Bashkatov, G.S. Terentyuk, A.B. Bucharskaya, G.N. Maslyakova, D.A. Gorin, V.V. Tuchin, G.B. Sukhorukov, *In vivo* optical monitoring of transcutaneous delivery of calcium carbonate microcontainers, Biomed. Opt Express 7 (2016) 2082, https://doi.org/10.1364/BOE.7.002082.
[91] S.R. Utz, G.B. Sukhorukov, V.V. Tuchin, D.A. Gorin, E.A. Genina, Y.I. Svenskaya, E.E. Talnikova, Targeted photosensitizer delivery: a prospective approach to vitiligo photochemotherapy, Vestn. Dermatol. Venerol. 95 (2019) 21–29, https://doi.org/10.25208/0042-4609-2019-95-1-21-29.
[92] Y.I. Svenskaya, E.E. Talnikova, B.V. Parakhonskiy, V.V. Tuchin, G.B. Sukhorukov, D.A. Gorin, S.R. Utz, Enhanced topical psoralen–ultraviolet A therapy via targeting to hair follicles, Br. J. Dermatol. 182 (2020) 1479–1481, https://doi.org/10.1111/bjd.18800.
[93] P. Zhao, M. Li, Y. Chen, C. He, X. Zhang, T. Fan, T. Yang, Y. Lu, R.J. Lee, X. Ma, J. Luo, G. Xiang, Selenium-doped calcium carbonate nanoparticles loaded with cisplatin enhance efficiency and reduce side effects, Int. J. Pharm. 570 (2019) 118638, https://doi.org/10.1016/j.ijpharm.2019.118638.
[94] D. Zhao, R.X. Zhuo, S.X. Cheng, Alginate modified nanostructured calcium carbonate with enhanced delivery efficiency for gene and drug delivery, Mol. Biosyst. 8 (2012) 753–759, https://doi.org/10.1039/c1mb05337j.
[95] Y. Zhao, Y. Lu, Y. Hu, J.-P. Li, L. Dong, L.-N. Lin, S.-H. Yu, Synthesis of superparamagnetic CaCO3 mesocrystals for multistage delivery in cancer therapy, Small 6 (2010) 2436–2442, https://doi.org/10.1002/smll.201000903.
[96] P. Decuzzi, S. Lee, B. Bhushan, M. Ferrari, A theoretical model for the margination of particles within blood vessels, Ann. Biomed. Eng. 33 (2005) 179–190, https://doi.org/10.1007/s10439-005-8976-5.